Chapter 3
The Theory of Electroweak Interactions

3.1 Introduction

In this chapter, we summarize the structure of the standard EW theory[1] and specify the couplings of the intermediate vector bosons $W^{\pm}$ and Z and those of the Higgs particle with the fermions and among themselves, as dictated by the gauge symmetry plus the observed matter content and the requirement of renormalizability. We discuss the realization of spontaneous symmetry breaking and the Higgs mechanism. We then review the phenomenological implications of the EW theory for collider physics, that is, we leave aside the classic low energy processes that are well described by the "old" weak interaction theory (see, for example, [148]).

For this discussion, we split the Lagrangian into two parts by separating the terms with the Higgs field:

$$\mathscr{L} = \mathscr{L}_{\text{gauge}} + \mathscr{L}_{\text{Higgs}} \,. \tag{3.1}$$

Both terms are written down as prescribed by the $SU(2) \bigotimes U(1)$ gauge symmetry and renormalizability, but the Higgs vacuum expectation value (VEV) induces the spontaneous symmetry breaking responsible for the non-vanishing vector boson and fermion masses.

[1] Some recent textbooks are listed in [276]. See also [34, 313].

G. Altarelli, *Collider Physics within the Standard Model*,
Lecture Notes in Physics 937, DOI 10.1007/978-3-319-51920-3_3

3.2 The Gauge Sector

We start by specifying $\mathscr{L}_{\text{gauge}}$, which involves only gauge bosons and fermions, according to the general formalism of gauge theories discussed in Chap. 1:

$$\mathscr{L}_{\text{gauge}} = -\frac{1}{4}\sum_{A=1}^{3} F^A_{\mu\nu}F^{A\mu\nu} - \frac{1}{4}B_{\mu\nu}B^{\mu\nu} + \bar{\psi}_{\text{L}}\text{i}\gamma^\mu D_\mu \psi_{\text{L}} + \bar{\psi}_{\text{R}}\text{i}\gamma^\mu D_\mu \psi_{\text{R}} \ . \tag{3.2}$$

This is the Yang–Mills Lagrangian for the gauge group $SU(2) \otimes U(1)$ with fermion matter fields. Here

$$B_{\mu\nu} = \partial_\mu B_\nu - \partial_\nu B_\mu \ , \qquad F^A_{\mu\nu} = \partial_\mu W^A_\nu - \partial_\nu W^A_\mu - g\epsilon_{ABC}\, W^B_\mu W^C_\nu \ , \tag{3.3}$$

are the gauge antisymmetric tensors constructed out of the gauge field B_μ associated with $U(1)$ and W^A_μ corresponding to the three $SU(2)$ generators, while ϵ_{ABC} are the group structure constants [see (3.5) and (3.6)], which, for $SU(2)$, coincide with the totally antisymmetric Levi-Civita tensor, with $\epsilon_{123} = 1$ (recall the familiar angular momentum commutators). The normalization of the $SU(2)$ gauge coupling g is therefore specified by (3.3).

As discussed in Sect. 1.5, the standard EW theory is a chiral theory, in the sense that ψ_{L} and ψ_{R} behave differently under the gauge group (so that parity and charge conjugation non-conservation are made possible in principle). Thus, mass terms for fermions (of the form $\bar{\psi}_{\text{L}}\psi_{\text{R}} + \text{h.c.}$) are forbidden in the symmetric limit. In the following, $\psi_{\text{L,R}}$ are column vectors, including all fermion types in the theory that span generic reducible representations of $SU(2) \otimes U(1)$.

In the absence of mass terms, there are only vector and axial vector interactions in the Lagrangian, and these have the property of not mixing ψ_{L} and ψ_{R}. Fermion masses will be introduced, together with $W^\pm$ and Z masses, by the mechanism of symmetry breaking. The covariant derivatives $D_\mu\psi_{\text{L,R}}$ are given explicitly by

$$D_\mu \psi_{\text{L,R}} = \left(\partial_\mu + \text{i}g\sum_{A=1}^{3} t^A_{\text{L,R}} W^A_\mu + \text{i}g'\frac{1}{2}Y_{\text{L,R}}B_\mu\right)\psi_{\text{L,R}} \ , \tag{3.4}$$

where $t^A_{\text{L,R}}$ and $Y_{\text{L,R}}/2$ are the $SU(2)$ and $U(1)$ generators, respectively, in the reducible representations $\psi_{\text{L,R}}$. The commutation relations of the $SU(2)$ generators are given by

$$\left[t^A_{\text{L}}, t^B_{\text{L}}\right] = \text{i}\epsilon_{ABC}t^C_{\text{L}} \ , \quad \left[t^A_{\text{R}}, t^B_{\text{R}}\right] = \text{i}\epsilon_{ABC}t^C_{\text{R}} \ . \tag{3.5}$$

We use the normalization in (1.11) [in the fundamental representation of $SU(2)$]. The electric charge generator Q (in units of e, the positron charge) is given by

$$Q = t_{\rm L}^3 + \frac{1}{2}Y_{\rm L} = t_{\rm R}^3 + \frac{1}{2}Y_{\rm R} \ . \tag{3.6}$$

Note that the normalization of the $U(1)$ gauge coupling g' in (3.4) is now specified as a consequence of (3.6). Note also that $t_{\rm R}^i \psi_{\rm R} = 0$, given that, for all known quarks and leptons, $\psi_{\rm R}$ is a singlet. But in the following, we keep $t_{\rm R}^i \psi_{\rm R}$ for generality, in case one day a non-singlet right-handed fermion is discovered.

3.3 Couplings of Gauge Bosons to Fermions

All fermion couplings of the gauge bosons can be derived directly from (3.2) and (3.4). The charged W_μ fields are described by $W_\mu^{1,2}$, while the photon A_μ and weak neutral gauge boson Z_μ are obtained from combinations of W_μ^3 and B_μ. The charged-current (CC) couplings are the simplest. One starts from the $W_\mu^{1,2}$ terms in (3.2) and (3.4), which can be written as

$$\begin{aligned} g(t^1 W_\mu^1 + t^2 W_\mu^2) &= g\left[\frac{1}{\sqrt{2}}(t^1 + {\rm i}t^2)\frac{1}{\sqrt{2}}(W_\mu^1 - {\rm i}W_\mu^2) + {\rm h.c.}\right] \\ &= g\left(\frac{1}{\sqrt{2}}t^+ W_\mu^- + {\rm h.c.}\right) \ , \end{aligned} \tag{3.7}$$

where $t^\pm = t^1 \pm {\rm i}t^2$ and $W^\pm = (W^1 \pm {\rm i}W^2)/\sqrt{2}$. By applying this generic relation to L and R fermions separately, we obtain the vertex

$$V_{\bar\psi\psi W} = g\bar\psi\gamma_\mu\left[\frac{1}{\sqrt{2}}t_{\rm L}^+\frac{1}{2}(1-\gamma_5) + \frac{1}{\sqrt{2}}t_{\rm R}^+\frac{1}{2}(1+\gamma_5)\right]\psi W_\mu^- + {\rm h.c.} \tag{3.8}$$

Given that $t_{\rm R} = 0$ for all fermions in the SM, the charged current is pure $V-A$. In the neutral current (NC) sector, the photon A_μ and the mediator Z_μ of the weak NC are orthogonal and normalized linear combinations of B_μ and W_μ^3:

$$\begin{aligned} A_\mu &= \cos\theta_{\rm W} B_\mu + \sin\theta_{\rm W} W_\mu^3 \ , \\ Z_\mu &= -\sin\theta_{\rm W} B_\mu + \cos\theta_{\rm W} W_\mu^3 \ , \end{aligned} \tag{3.9}$$

whence

$$\begin{aligned} W_\mu^3 &= \sin\theta_{\rm W} A_\mu + \cos\theta_{\rm W} Z_\mu \ , \\ B_\mu &= \cos\theta_{\rm W} A_\mu - \sin\theta_{\rm W} Z_\mu \ . \end{aligned} \tag{3.10}$$

Equations (3.9) define the weak mixing angle $\theta_{\rm W}$. We can rewrite the W^3_μ and B_μ terms in (3.2) and (3.4) as follows:

$$gt^3 W^3_\mu + \frac{1}{2} g' Y B_\mu = \left[gt^3 \sin\theta_{\rm W} + g'(Q - t^3)\cos\theta_{\rm W} \right] A_\mu + \left[gt^3 \cos\theta_{\rm W} - g'(Q - t^3)\sin\theta_{\rm W} \right] Z_\mu \,, \tag{3.11}$$

where (3.6) was also used for the charge matrix Q. The photon is characterized by equal couplings to left and right fermions, with a strength equal to the electric charge. Thus we immediately obtain

$$g \sin\theta_{\rm W} = g' \cos\theta_{\rm W} = e \,, \tag{3.12}$$

so that

$$\tan\theta_{\rm W} = g'/g \,. \tag{3.13}$$

Once $\theta_{\rm W}$ has been fixed by the photon couplings, it is a matter of simple algebra to derive the Z couplings, with the result

$$V_{\bar\psi\psi Z} = \frac{g}{2\cos\theta_{\rm W}} \bar\psi \gamma_\mu \left[t^3_{\rm L}(1 - \gamma_5) + t^3_{\rm R}(1 + \gamma_5) - 2Q \sin^2\theta_{\rm W} \right] \psi Z^\mu \,, \tag{3.14}$$

where $V_{\bar\psi\psi Z}$ is a notation for the vertex. Once again, recall that in the minimal SM, $t^3_{\rm R} = 0$ and $t^3_{\rm L} = \pm 1/2$.

In order to derive the effective four-fermion interactions, which are equivalent at low energies to the CC and NC couplings given in (3.8) and (3.14), we anticipate that large masses, as observed experimentally, are provided for $W^\pm$ and Z by $\mathscr{L}_{\rm Higgs}$. For left–left CC couplings, when the square of the momentum transfer can be neglected (in comparison with m^2_W) in the propagator of Born diagrams with single W exchange (see, for example, the diagram for μ decay in Fig. 3.1), Eq. (3.8) implies

$$\mathscr{L}^{\rm C}_{\rm eff} \simeq \frac{g^2}{8 m^2_W} \left[\bar\psi \gamma_\mu (1 - \gamma_5) t^+_{\rm L} \psi \right] \left[\bar\psi \gamma^\mu (1 - \gamma_5) t^-_{\rm L} \psi \right] . \tag{3.15}$$

By specializing further in the case of doublet fields, such as $\nu_e - e^-$ or $\nu_\mu - \mu^-$, we obtain the tree-level relation of g with the Fermi coupling constant $G_{\rm F}$ precisely

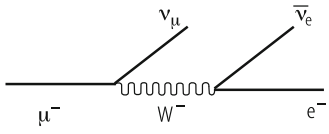

Fig. 3.1 Born diagram for μ decay

measured from μ decay [see (1.2) and (1.3)]:

$$\frac{G_{\rm F}}{\sqrt{2}} = \frac{g^2}{8m_W^2} \,. \tag{3.16}$$

Recalling that $g \sin\theta_{\rm W} = e$, we can also cast this relation in the form

$$m_W = \frac{\mu_{\rm Born}}{\sin\theta_{\rm W}} \,, \tag{3.17}$$

with

$$\mu_{\rm Born} = \left(\frac{\pi\alpha}{\sqrt{2}G_{\rm F}}\right)^{1/2} \simeq 37.2802\,{\rm GeV}\,, \tag{3.18}$$

where α is the QED fine-structure constant ($\alpha \equiv e^2/4\pi = 1/137.036$).

In the same way, for neutral currents, in the Born approximation, (3.14) yields the effective four-fermion interaction:

$$\mathscr{L}_{\rm eff}^{\rm NC} \simeq \sqrt{2}\, G_{\rm F}\rho_0 \bar{\psi}\gamma_\mu[\ldots]\psi\bar{\psi}\gamma^\mu[\ldots]\psi \,, \tag{3.19}$$

where

$$[\ldots] \equiv t_{\rm L}^3(1-\gamma_5) + t_{\rm R}^3(1+\gamma_5) - 2Q\sin^2\theta_{\rm W} \tag{3.20}$$

and

$$\rho_0 = \frac{m_W^2}{m_Z^2\cos^2\theta_{\rm W}} \,. \tag{3.21}$$

All couplings given in this section are valid at tree level, and are modified in higher orders of perturbation theory. In particular, the relations between m_W and $\sin\theta_{\rm W}$ [(3.17) and (3.18)] and the observed values of ρ ($\rho = \rho_0$ at tree level) in different NC processes, are altered by computable EW radiative corrections, as discussed in Sect. 3.11.

The partial width $\Gamma(W \to \bar{f}f')$ is given in the Born approximation by the simplest diagram in Fig. 3.2, and with $t_{\rm R} = 0$, one readily obtains from (3.8), in the limit of

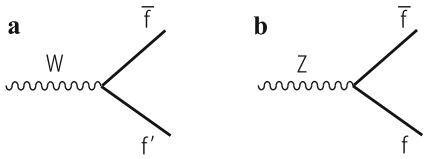

Fig. 3.2 Diagrams for (**a**) the W and (**b**) the Z widths in the Born approximation

neglecting the fermion masses and summing over all possible f' for a given f,

$$\Gamma(W \to \bar{f}f') = N_{\rm C}\frac{G_{\rm F}m_W^3}{6\pi\sqrt{2}} = N_{\rm C}\frac{\alpha m_W}{12\sin^2\theta_{\rm W}}\,, \tag{3.22}$$

where $N_{\rm C} = 3$ or 1 is the number of colours for quarks or leptons, respectively, and (3.12) and (3.16) have been used. Here and in the following expressions for the Z widths, the one-loop QCD corrections for the quark channels can be absorbed in a redefinition of $N_{\rm C}$:

$$N_{\rm C} \to 3\big[1 + \alpha_{\rm s}(m_Z)/\pi + \cdots\big]\,.$$

Note that the widths are particularly large because the rate already occurs at order g^2 or $G_{\rm F}$. The experimental values of the total W width and the leptonic branching ratio (the average of e, μ, and τ modes) are [307, 350] (see Sect. 3.11):

$$\Gamma_W = 2.085 \pm 0.042\,{\rm GeV}\,, \qquad B(W \to l\nu_l) = 10.80 \pm 0.09\,. \tag{3.23}$$

The branching ratio B is in very good agreement with the simple approximate formula, derived from (3.22):

$$B(W \to l\nu_l) \sim \frac{1}{2\times 3\times\big[1+\alpha_{\rm s}(m_Z^2)/\pi\big]+3} \sim 10.8\%\,. \tag{3.24}$$

The denominator corresponds to the sum of the final states $d'\bar{u}$, $s'\bar{c}$, $e^-\bar{\nu}_e$, $\mu^-\bar{\nu}_\mu$, $\tau^-\bar{\nu}_\tau$, where d' and s' are defined in (3.63).

For $t_{\rm R} = 0$, the Z coupling to fermions in (3.14) can be cast into the form

$$V_{\bar{\psi}_f\psi_f Z} = \frac{g}{2\cos\theta_{\rm W}}\bar{\psi}_f\gamma_\mu\big[g_{\rm V}^f - g_{\rm A}^f\gamma_5\big]\psi_f Z^\mu\,, \tag{3.25}$$

with

$$g_{\rm A}^f = t_{\rm L}^{3f}\,, \quad g_{\rm V}^f/g_{\rm A}^f = 1 - 4|Q_f|\sin^2\theta_{\rm W}\,, \tag{3.26}$$

and $t_{\rm L}^{3f} = \pm 1/2$ for up-type or down-type fermions. In terms of $g_{\rm A,V}$ given in (3.26) (the widths are proportional to $g_{\rm V}^2 + g_{\rm A}^2$), for negligible fermion masses, the partial width $\Gamma(Z \to \bar{f}f)$ in the Born approximation (see the diagram in Fig. 3.2) is given by

$$\begin{aligned}\Gamma(Z \to \bar{f}f) &= N_{\rm C}\frac{\alpha m_Z}{12\sin^2 2\theta_{\rm W}}\big[1 + (1 - 4|Q_f|\sin^2\theta_{\rm W})^2\big] \\ &= N_{\rm C}\rho_0\frac{G_{\rm F}m_Z^3}{24\pi\sqrt{2}}\big[1 + (1 - 4|Q_f|\sin^2\theta_{\rm W})^2\big]\,,\end{aligned} \tag{3.27}$$

where $\rho_0 = m_W^2/m_Z^2 \cos^2\theta_W$ is given in (3.52). The experimental values of the total Z width and the partial rates into charged leptons (average of e, μ, and τ), into hadrons and into invisible channels are [307, 350]

$$\begin{aligned} \Gamma_Z &= 2.4952 \pm 0.0023\,\text{GeV}\,, \quad \Gamma_{l^+l^-} = 83.984 \pm 0.086\,\text{MeV}\,, \\ \Gamma_h &= 1744.4 \pm 2.0\,\text{MeV}\,, \quad \Gamma_{\text{inv}} = 499.0 \pm 1.5\,\text{MeV}\,. \end{aligned} \tag{3.28}$$

The measured value of the Z invisible width, taking radiative corrections into account, leads to the determination of the number of light active neutrinos [307, 350]:

$$N_\nu = 2.9840 \pm 0.0082\,, \tag{3.29}$$

well compatible with the three known neutrinos ν_e, ν_μ, and ν_τ. Hence, there exist only the three known sequential generations of fermions (with light neutrinos), a result which also has important consequences in astrophysics and cosmology.

At the Z peak, besides total cross-sections, various types of asymmetries have been measured. The results of all asymmetry measurements are quoted in terms of the asymmetry parameter A_f, defined in terms of the effective coupling constants, g_V^f and g_A^f, as

$$A_f = 2\frac{g_V^f g_A^f}{g_V^{f2} + g_A^{f2}} = 2\frac{g_V^f/g_A^f}{1 + (g_V^f/g_A^f)^2}\,, \qquad A_{FB}^f = \frac{3}{4}A_e A_f\,. \tag{3.30}$$

The measurements are the forward–backward asymmetry ($A_{FB}^f = 3A_e A_f/4$), the tau polarization (A_τ) and its forward–backward asymmetry (A_e) measured at LEP, and also the left–right and left–right forward–backward asymmetry measured at SLC (A_e and A_f, respectively). Hence, the set of partial width and asymmetry results allows the extraction of the effective coupling constants: widths measure $(g_V^2 + g_A^2)$ and asymmetries measure g_V/g_A.

The top quark is heavy enough to be able to decay into a real bW pair, which is by far its dominant decay channel. The next mode, $t \to sW$, is suppressed in rate by a factor $|V_{ts}|^2 \sim 1.7 \times 10^{-3}$ [see (3.68)–(3.70)]. The associated width, neglecting m_b effects but including 1-loop QCD corrections in the limit $m_W = 0$, is given by (we have omitted a factor $|V_{tb}|^2$ that we set equal to 1) [253]

$$\Gamma(t \to bW^+) = \frac{G_F m_t^3}{8\pi\sqrt{2}}\left(1 - \frac{m_W^2}{m_t^2}\right)^2\left(1 + 2\frac{m_W^2}{m_t^2}\right)\left[1 - \frac{2\alpha_s(m_Z)}{3\pi}\left(\frac{2\pi^2}{3} - \frac{5}{2}\right) + \cdots\right]. \tag{3.31}$$

The top quark lifetime is so short, about 0.5×10^{-24} s, that it decays before hadronizing or forming toponium bound states.

3.4 Gauge Boson Self-Interactions

The gauge boson self-interactions can be derived from the $F_{\mu\nu}$ term in $\mathscr{L}_{\text{gauge}}$ using (3.9) and $W^{\pm} = (W^1 \pm \mathrm{i}W^2)/\sqrt{2}$. Defining the three-gauge-boson vertex as in Fig. 3.3 (with all incoming lines), we obtain

$$V_{W^-W^+V} = \mathrm{i}g_{W^-W^+V}\left[g_{\mu\nu}(p-q)_\lambda + g_{\mu\lambda}(r-p)_\nu + g_{\nu\lambda}(q-r)_\mu\right], \tag{3.32}$$

with $V \equiv \gamma, Z$ and

$$g_{W^-W^+\gamma} = g\sin\theta_{\mathrm{W}} = e\,, \qquad g_{W^-W^+Z} = g\cos\theta_{\mathrm{W}}\,. \tag{3.33}$$

Note that the photon coupling to the W is fixed by the electric charge, as imposed by QED gauge invariance. The ZWW coupling is larger by a factor of $\cot\theta_{\mathrm{W}}$. This form of the triple gauge vertex is very special: in general, there could be departures from the above SM expression, even if we restrict to Lorentz invariant, electromagnetic gauge symmetric, and C and P conserving couplings. In fact, some small corrections are already induced by the radiative corrections. But, in principle, the modifications induced by some new physics effect could be more important. The experimental testing of the triple gauge vertices has been done in the past, mainly at LEP2 and at the Tevatron [235], and now also at the LHC [319].

As a particularly important example, the cross-section and angular distributions for the process $e^+e^- \to W^+W^-$ have been studied at LEP2. In the Born approximation, the Feynman diagrams for the LEP2 process are shown in Fig. 3.4 [46]. Besides neutrino exchange, which only involves the well established charged

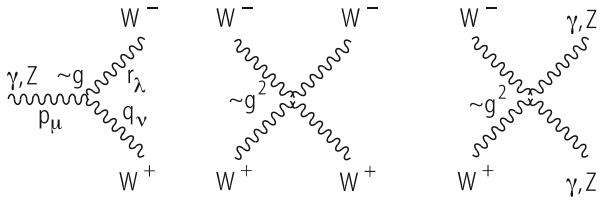

Fig. 3.3 The 3- and 4-gauge boson vertices. The cubic coupling is of order g and the quartic coupling of order g^2

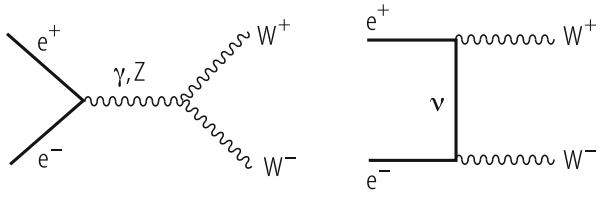

Fig. 3.4 Lowest order diagrams for $e^+e^- \to W^+W^-$

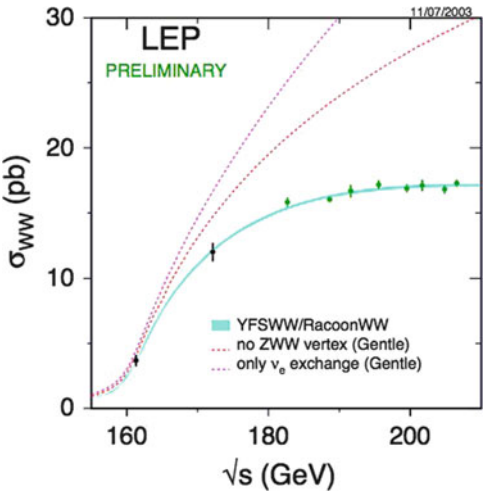

Fig. 3.5 Measured production cross-section for $e^+e^- \to W^+W^-$ compared to the SM and fictitious theories, not including trilinear gauge couplings, as indicated. From [281]

current vertex, the triple weak gauge vertices $V_{W^-W^+V}$ appear in the γ and Z exchange diagrams. The Higgs exchange is negligible because the electron mass is very small. The analytic cross-section formula in the Born approximation can be found, for example, in [307] (in the section entitled *Cross-section formulae for specific processes*). The experimental data are compared with the SM prediction in Fig. 3.5. Within the present accuracy, the agreement is good. Note that the sum of all three exchange amplitudes has a better high energy behaviour than its individual components. This is due to cancellations among the amplitudes implied by gauge invariance, connected to the fact that the theory is renormalizable (the cross-section can be seen as a contribution to the imaginary part of the $e^+e^- \to e^+e^-$ amplitude).

The quartic gauge coupling is proportional to $g^2\epsilon_{ABC}W^BW^C\epsilon_{ADE}W^DW^E$. Thus in the term with $A = 3$, we have four charged W particles. For $A = 1$ or 2, we have two charged W particles and two W^3 particles, each W_3 being a combination of γ and Z according to (3.10). With a little algebra the quartic vertex can be cast in the form

$$V_{WWVV} = \mathrm{i}g_{WWVV}\left(2g_{\mu\nu}g_{\lambda\rho} - g_{\mu\lambda}g_{\nu\rho} - g_{\mu\rho}g_{\nu\lambda}\right) , \tag{3.34}$$

where μ and ν refer to W^+W^+ in the $4W$ vertex and to VV in the $WWVV$ case, and

$$g_{WWWW} = g^2 , \quad g_{WW\gamma\gamma} = -e^2 , \quad g_{WW\gamma Z} = -eg\cos\theta_\mathrm{W} , \quad g_{WWZZ} = -g^2\cos^2\theta_\mathrm{W} . \tag{3.35}$$

In order to obtain these results for the vertex, the reader must duly take into account the factor of $-1/4$ in front of $F^2_{\mu\nu}$ in the Lagrangian and the statistical factors which are equal to 2 for each pair of identical particles (like W^+W^+ or $\gamma\gamma$, for example). As the quartic coupling is quadratic in g and hence small, it has not yet been possible to test it directly.

3.5 The Higgs Sector

We now turn to the Higgs sector of the EW Lagrangian [243]. Until recently, this simplest realization of the EW symmetry breaking was a pure conjecture. But in July 2012 the ATLAS and CMS Collaborations at the CERN LHC announced [2, 135] the discovery of a particle with mass $m_{\rm H} \sim 126\,{\rm GeV}$ that looks very much like the long sought Higgs particle. More precise measurements of its couplings and the proof that its spin is zero are necessary before the identification with the SM Higgs boson can be completely established. But the following description of the Higgs sector of the SM can now be read with this striking development in mind.

The Higgs Lagrangian is specified by the gauge principle and the requirement of renormalizability to be

$$\mathscr{L}_{\rm Higgs} = (D_\mu \phi)^\dagger (D^\mu \phi) - V(\phi^\dagger \phi) - \bar{\psi}_{\rm L} \Gamma \psi_{\rm R} \phi - \bar{\psi}_{\rm R} \Gamma^\dagger \psi_{\rm L} \phi^\dagger \,, \tag{3.36}$$

where ϕ is a column vector including all Higgs fields which generally transforms as a reducible representation of the gauge group $SU(2)_{\rm L} \otimes U(1)$. In the minimal SM, it is just a complex doublet. The quantities Γ (which include all coupling constants) are matrices that make the Yukawa couplings invariant under the Lorentz and gauge groups. The potential $V(\phi^\dagger \phi)$, symmetric under $SU(2)_{\rm L} \otimes U(1)$, contains at most quartic terms in ϕ so that the theory is renormalizable:

$$V(\phi^\dagger \phi) = -\mu^2 \phi^\dagger \phi + \frac{1}{2} \lambda (\phi^\dagger \phi)^2 \tag{3.37}$$

As discussed in Chap. 1, spontaneous symmetry breaking is induced if the minimum of V, which is the classical analogue of the quantum mechanical vacuum state, is not a single point but a whole orbit obtained for non-vanishing ϕ values. Precisely, we denote the vacuum expectation value (VEV) of ϕ, i.e., the position of the minimum, by v (which is a doublet):

$$\langle 0 | \phi(x) | 0 \rangle = v = \begin{pmatrix} 0 \\ v \end{pmatrix} \neq 0 \,. \tag{3.38}$$

The reader should be careful that, for economy of notation, the same symbol is used for the doublet and for the only nonzero component of the same doublet. The fermion mass matrix is obtained from the Yukawa couplings by replacing $\phi(x)$ by v :

$$M = \bar{\psi}_{\rm L} \mathscr{M} \psi_{\rm R} + \bar{\psi}_{\rm R} \mathscr{M}^\dagger \psi_{\rm L} \,, \tag{3.39}$$

with

$$\mathscr{M} = \Gamma v \,. \tag{3.40}$$

In the MSM, where all left fermions $\psi_{\rm L}$ are doublets and all right fermions $\psi_{\rm R}$ are singlets, only Higgs doublets can contribute to fermion masses. There are enough free couplings in Γ to ensure that a single complex Higgs doublet is indeed sufficient to generate the most general fermion mass matrix. It is important to observe that, by a suitable change of basis, we can always make the matrix $\mathscr{M}$ Hermitian (so that the mass matrix is γ_5-free) and diagonal. In fact, we can make separate unitary transformations on $\psi_{\rm L}$ and $\psi_{\rm R}$ according to

$$\psi'_{\rm L} = U\psi_{\rm L} \ , \quad \psi'_{\rm R} = W\psi_{\rm R} \ , \tag{3.41}$$

and consequently,

$$\mathscr{M} \to \mathscr{M}' = U^\dagger \mathscr{M} W \ . \tag{3.42}$$

This transformation produces different effects on mass terms and on the structure of the fermion couplings in $\mathscr{L}_{\rm symm}$, because both the kinetic terms and the couplings to gauge bosons do not mix L and R spinors. The combined effect of these unitary rotations leads to the phenomenon of mixing and, generically, to flavour-changing neutral currents (FCNC), as we shall see in Sect. 3.6.

If only one Higgs doublet is present, the change of basis that makes $\mathscr{M}$ diagonal will at the same time diagonalize the fermion–Higgs Yukawa couplings. Thus, in this case, no flavour-changing neutral Higgs vertices are present. This is not true, in general, when there are several Higgs doublets. But one Higgs doublet for each electric charge sector, i.e., one doublet coupled only to u-type quarks, one doublet to d-type quarks, one doublet to charged leptons, and possibly one for neutrino Dirac masses, would also be acceptable, because the mass matrices of fermions with different charges are diagonalized separately. For several Higgs doublets in a given charge sector, it is also possible to generate CP violation by complex phases in the Higgs couplings. In the presence of six quark flavours, this CP violation mechanism is not necessary. In fact, at the moment, the simplest model with only one Higgs doublet could be adequate for describing all observed phenomena.

We now consider the gauge boson masses and their couplings to the Higgs. These effects are induced by the $(D_\mu\phi)^\dagger(D^\mu\phi)$ term in $\mathscr{L}_{\rm Higgs}$ [see (3.36)], where

$$D_\mu\phi = \left(\partial_\mu + {\rm i}g\sum_{A=1}^{3} t^A W_\mu^A + {\rm i}g'\frac{Y}{2}B_\mu\right)\phi \ . \tag{3.43}$$

Here t^A and $Y/2$ are the $SU(2)\otimes U(1)$ generators in the reducible representation spanned by ϕ. Not only doublets, but all non-singlet Higgs representations can contribute to gauge boson masses. The condition that the photon remain massless is equivalent to the condition that the vacuum be electrically neutral:

$$Q|v\rangle = \left(t^3 + \frac{1}{2}Y\right)|v\rangle = 0 \ . \tag{3.44}$$

We now explicitly consider the case of a single Higgs doublet:

$$\phi = \begin{pmatrix} \phi^+ \\ \phi^0 \end{pmatrix} , \qquad v = \begin{pmatrix} 0 \\ v \end{pmatrix} . \tag{3.45}$$

The charged W mass is given by the quadratic terms in the W field arising from $\mathscr{L}_{\text{Higgs}}$, when $\phi(x)$ is replaced by v in (3.38). Recalling (3.7), we obtain

$$m_W^2 W_\mu^+ W^{-\mu} = g^2 \left| t^+ v/\sqrt{2} \right|^2 W_\mu^+ W^{-\mu} , \tag{3.46}$$

whilst for the Z mass we get [recalling (3.9)–(3.11)]

$$\frac{1}{2} m_Z^2 Z_\mu Z^\mu = \left| \left(g t^3 \cos\theta_{\text{W}} - g' \frac{Y}{2} \sin\theta_{\text{W}} \right) v \right|^2 Z_\mu Z^\mu , \tag{3.47}$$

where the factor of 1/2 on the left-hand side is the correct normalization for the definition of the mass of a neutral field. Using (3.44), relating the action of t^3 and $Y/2$ on the vacuum v, and (3.13), we obtain

$$\frac{1}{2} m_Z^2 = (g \cos\theta_{\text{W}} + g' \sin\theta_{\text{W}})^2 |t^3 v|^2 = \frac{g^2}{\cos^2\theta_{\text{W}}} |t^3 v|^2 . \tag{3.48}$$

For a Higgs doublet, as in (3.45), we have

$$|t^+ v|^2 = v^2 , \qquad |t^3 v|^2 = 1/4 v^2 , \tag{3.49}$$

so that

$$m_W^2 = \frac{1}{2} g^2 v^2 , \qquad m_Z^2 = \frac{g^2 v^2}{2 \cos^2\theta_{\text{W}}} . \tag{3.50}$$

Note that by using (3.16), we obtain

$$v = 2^{-3/4} G_{\text{F}}^{-1/2} = 174.1\,\text{GeV} . \tag{3.51}$$

It is also evident that, for Higgs doublets,

$$\rho_0 = \frac{m_W^2}{m_Z^2 \cos^2\theta_{\text{W}}} = 1 . \tag{3.52}$$

This relation is typical of one or more Higgs doublets and would be spoiled by the existence of Higgs triplets, etc. In general,

$$\rho_0 = \frac{\sum_i \left[(t_i)^2 - (t_i^3)^2 + t_i \right] v_i^2}{\sum_i 2 (t_i^3)^2 v_i^2} , \tag{3.53}$$

for several Higgs bosons with VEVs v_i, weak isospins t_i, and z-components t_i^3. These results are valid at the tree level and are modified by calculable EW radiative corrections, as discussed in Sect. 3.11.

The measured values of the W (combined from the LEP and Tevatron experiments) and Z masses (from LEP) are [307, 350]:

$$m_W = 80.385 \pm 0.015\,\text{GeV}\,, \qquad m_Z = 91.1876 \pm 0.0021\,\text{GeV}\,. \tag{3.54}$$

In the minimal version of the SM, only one Higgs doublet is present. Then the fermion–Higgs couplings are in proportion to the fermion masses. In fact, from the fermion f Yukawa couplings $g_{\phi\bar{f}f}(\bar{f}_\text{L}\phi f_\text{R} + \text{h.c.})$, the mass m_f is obtained by replacing ϕ by v, so that $m_f = g_{\phi\bar{f}f}v$. In the minimal SM, three out of the four Hermitian fields are removed from the physical spectrum by the Higgs mechanism and become the longitudinal modes of W^+, W^-, and Z. The fourth neutral Higgs is physical and should presumably be identified with the newly discovered particle at $\sim$126 GeV. If more doublets are present, two more charged and two more neutral Higgs scalars should be around for each additional doublet.

The couplings of the physical Higgs H can be simply obtained from $\mathscr{L}_\text{Higgs}$, by making the replacement (the remaining three Hermitian fields correspond to the would-be Goldstone bosons that become the longitudinal modes of $W^\pm$ and Z):

$$\phi(x) = \begin{pmatrix} \phi^+(x) \\ \phi^0(x) \end{pmatrix} \longrightarrow \begin{pmatrix} 0 \\ v + H/\sqrt{2} \end{pmatrix}\,, \tag{3.55}$$

so that $(D_\mu\phi)^\dagger(D^\mu\phi) = \partial_\mu H)^2/2 + \cdots$, with the results

$$\begin{aligned} \mathscr{L}[H,W,Z] = {} & g^2\frac{v}{\sqrt{2}}W_\mu^+W^{-\mu}H + \frac{g^2}{4}W_\mu^+W^{-\mu}H^2 \\ & + g^2\frac{v}{2\sqrt{2}\cos^2\theta_\text{W}}Z_\mu Z^\mu H + \frac{g^2}{8\cos^2\theta_\text{W}}Z_\mu Z^\mu H^2\,. \end{aligned} \tag{3.56}$$

Note that the trilinear couplings are nominally of order g^2, but the dimensionless coupling constant is actually of order g if we express the couplings in terms of the masses according to (3.50):

$$\begin{aligned} \mathscr{L}[H,W,Z] = {} & gm_W W_\mu^+W^{-\mu}H + \frac{g^2}{4}W_\mu^+W^{-\mu}H^2 \\ & + \frac{gm_Z}{2\cos^2\theta_\text{W}}Z_\mu Z^\mu H + \frac{g^2}{8\cos^2\theta_\text{W}}Z_\mu Z^\mu H^2\,. \end{aligned} \tag{3.57}$$

Thus the trilinear couplings of the Higgs to the gauge bosons are also proportional to the masses at fixed g [if instead G_F is kept fixed then, by (3.16), g is proportional to m_W, and the Higgs couplings are quadratic in m_W]. The quadrilinear couplings

are of order g^2. Recall that, to go from the Lagrangian to the Feynman rules for the vertices, the statistical factors must be taken into account. For example, the Feynman rule for the $ZZHH$ vertex is $ig_{\mu\nu}g^2/2\cos^2\theta_W$.

The generic coupling of H to a fermion of type f is given after diagonalization by

$$\mathscr{L}[H,\bar{\psi},\psi] = \frac{g_f}{\sqrt{2}}\bar{\psi}\psi H\ , \tag{3.58}$$

with

$$\frac{g_f}{\sqrt{2}} = \frac{m_f}{\sqrt{2}v} = 2^{1/4}G_F^{1/2}m_f\ . \tag{3.59}$$

The Higgs self-couplings are obtained from the potential in (3.37) by the replacement in (3.55). From the minimum condition

$$v = \sqrt{\frac{\mu^2}{\lambda}}\ , \tag{3.60}$$

one obtains

$$V = -\mu^2\left(v+\frac{H}{\sqrt{2}}\right)^2 + \frac{\mu^2}{2v^2}\left(v+\frac{H}{\sqrt{2}}\right)^4 = -\frac{\mu^2v^2}{2} + \mu^2H^2 + \frac{\mu^2}{\sqrt{2}v}H^3 + \frac{\mu^2}{8v^2}H^4\ , \tag{3.61}$$

The constant term can be omitted in our context. We see that the Higgs mass is positive [compare with (3.37)] and is given by

$$m_H^2 = 2\mu^2 = 2\lambda v^2\ . \tag{3.62}$$

By recalling the value of v in (3.51), we see that, for $m_H \sim 126\,\text{GeV}$, λ is small, in fact, $\lambda/2 \sim 0.13$. Note that $\lambda/2$ is the coefficient of ϕ^4 in (3.37), and the Higgs self-interaction is in the perturbative domain.

The difficulty in the Higgs search is due to the fact that it is heavy and coupled in proportion to mass: it is a heavy particle that must be radiated by another heavy particle. So a lot of phase space and luminosity are needed. At LEP2, the main process for Higgs production was the Higgs strahlung process $e^+e^- \to ZH$ shown in Fig. 3.6 [181]. The alternative process $e^+e^- \to H\nu\bar{\nu}$, via WW fusion, also shown in Fig. 3.6 [44], has a smaller cross-section at LEP2 energies, but would become important, even dominant, in higher energy e^+e^- colliders, like the ILC or CLIC (the corresponding ZZ fusion process has a much smaller cross-section). The analytic formulae for the cross-sections of both processes can be found, for example, in [46]. The direct experimental limit on m_H from LEP2 was $m_H \gtrsim 114\,\text{GeV}$ at 95% confidence level. The phenomenology of the SM Higgs particle and its production and detection at hadron colliders will be discussed in Sects. 3.13 and 3.16.

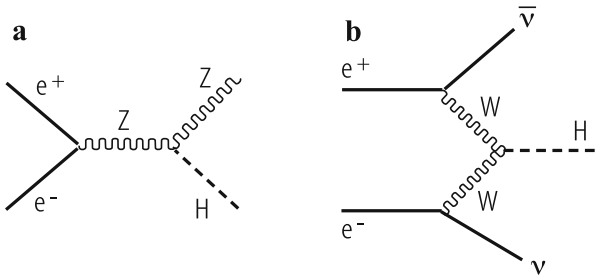

Fig. 3.6 Higgs production diagrams in the Born approximation for e^+e^- annihilation: (**a**) The Higgs strahlung process $e^+e^- \to ZH$, (**b**) the WW fusion process $e^+e^- \to H\nu\bar{\nu}$

3.6 The CKM Matrix and Flavour Physics

Weak charged current vertices are the only tree level interactions in the SM that change flavour. For example, by emission of a W^+, an up-type quark is turned into a down-type quark, or a ν_l neutrino is turned into a l^- charged lepton (all fermions are left-handed). If we start from an up quark that is a mass eigenstate, emission of a W^+ turns it into a down-type quark state d' (the weak isospin partner of u) which is not in general a mass eigenstate. The mass eigenstates and the weak eigenstates do not coincide, and a unitary transformation connects the two sets:

$$D' = \begin{pmatrix} d' \\ s' \\ b' \end{pmatrix} = V \begin{pmatrix} d \\ s \\ b \end{pmatrix} = VD \,, \tag{3.63}$$

where V is the Cabibbo–Kobayashi–Maskawa (CKM) matrix [121]. By analogy with D, we let U denote the column vector of the three up-quark mass eigenstates. Thus, in terms of mass eigenstates, the charged weak current of quarks is of the form

$$J_\mu^+ \propto \bar{U}\gamma_\mu(1-\gamma_5)t^+VD \,, \tag{3.64}$$

where

$$V = U_u^\dagger U_d \,. \tag{3.65}$$

Here U_u and U_d are the unitary matrices that operate on left-handed doublets in the diagonalization of the u and d quarks, respectively [see (3.41)]. Since V is unitary (i.e., $VV^\dagger = V^\dagger V = 1$) and commutes with T^2, T_3 and Q (because all d-type quarks have the same isospin and charge), the neutral current couplings are diagonal in both the primed and the unprimed basis. [If the down-type quark terms in the Z current are written in terms of weak isospin eigenvectors as $\bar{D}'\Gamma D'$, then by changing basis we get $\bar{D}V^\dagger\Gamma VD$, and V and Γ commute because, as can be seen from (3.20), Γ is made

of Dirac matrices and T_3 and Q generator matrices.] It follows that $\bar{D}'\Gamma D' = \bar{D}\Gamma D$. This is the GIM mechanism [226], which ensures natural flavour conservation of the neutral current couplings at the tree level.

For N generations of quarks, V is a $N \times N$ unitary matrix that depends on N^2 real numbers (N^2 complex entries with N^2 unitarity constraints). However, the $2N$ phases of up- and down-type quarks are not observable. Note that an overall phase drops away from the expression of the current in (3.64), so that only $2N-1$ phases can affect V. In total, V depends on $N^2-2N+1 = (N-1)^2$ real physical parameters. Similar counting gives $N(N-1)/2$ as the number of independent parameters in an orthogonal $N \times N$ matrix. This implies that in V we have $N(N-1)/2$ mixing angles and $(N-1)^2 - N(N-1)/2 = (N-1)(N-2)/2$ phases: for $N = 2$, one mixing angle (the Cabibbo angle θ_C) and no phases, for $N = 3$ three angles (θ_{12}, θ_{13}, and θ_{23}) and one phase φ, and so on.

Given the experimentally near-diagonal structure of V, a convenient parametrization is the one proposed by Maiani [286]. It can be cast in the form of a product of three independent 2×2 block matrices (s_{ij} and c_{ij} are shorthands for $\sin\theta_{ij}$ and $\cos\theta_{ij}$):

$$V = \begin{pmatrix} 1 & 0 & 0 \\ 0 & c_{23} & s_{23} \\ 0 & -s_{23} & c_{23} \end{pmatrix} \begin{pmatrix} c_{13} & 0 & s_{13}\mathrm{e}^{\mathrm{i}\varphi} \\ 0 & 1 & 0 \\ -s_{13}\mathrm{e}^{-\mathrm{i}\varphi} & 0 & c_{13} \end{pmatrix} \begin{pmatrix} c_{12} & s_{12} & 0 \\ -s_{12} & c_{12} & 0 \\ 0 & 0 & 1 \end{pmatrix} . \tag{3.66}$$

The advantage of this parametrization is that the three mixing angles are of different orders of magnitude. In fact, from experiment we know that $s_{12} \equiv \lambda$, $s_{23} \sim O(\lambda^2)$, and $s_{13} \sim O(\lambda^3)$, where $\lambda = \sin\theta_C$ is the sine of the Cabibbo angle, and, as an order of magnitude, s_{ij} can be expressed in terms of small powers of λ. More precisely, following Wolfenstein [370], one can set

$$s_{12} \equiv \lambda \,, \qquad s_{23} = A\lambda^2 \,, \qquad s_{13}\mathrm{e}^{-\mathrm{i}\phi} = A\lambda^3(\rho - \mathrm{i}\eta) \,. \tag{3.67}$$

As a result, by neglecting terms of higher order in λ, one can write

$$V = \begin{bmatrix} V_{ud} & V_{us} & V_{ub} \\ V_{cd} & V_{cs} & V_{cb} \\ V_{td} & V_{ts} & V_{tb} \end{bmatrix} \sim \begin{bmatrix} 1-\lambda^2/2 & \lambda & A\lambda^3(\rho - \mathrm{i}\eta) \\ -\lambda & 1-\lambda^2/2 & A\lambda^2 \\ A\lambda^3(1-\rho-\mathrm{i}\eta) & -A\lambda^2 & 1 \end{bmatrix} + O(\lambda^4). \tag{3.68}$$

It has become customary to make the replacement $\rho, \eta \to \bar{\rho}, \bar{\eta}$ with

$$\rho - \mathrm{i}\eta = \frac{\bar{\rho} - \mathrm{i}\bar{\eta}}{\sqrt{1-\lambda^2}} \sim (\bar{\rho} - \mathrm{i}\bar{\eta})\left(1 + \frac{\lambda^2}{2} + \cdots\right) . \tag{3.69}$$

The best values of the CKM parameters as obtained from experiment are continuously updated in [344, 355] (a survey of the current status of the CKM parameters can also be found in [307]). A Summer 2013 fit [355] led to the values

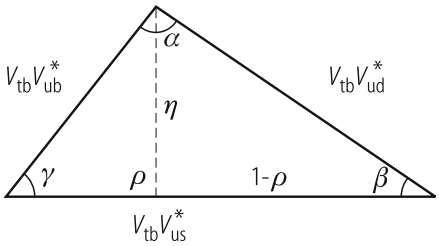

Fig. 3.7 The unitarity triangle corresponding to (3.71)

(compatible values, within stated errors, are given in [344]):

$$\begin{aligned} \lambda &= 0.22535 \pm 0.00065\,, \qquad A = 0.822 \pm 0.012\,, \\ \bar{\rho} &= 0.127 \pm 0.023\,, \qquad \bar{\eta} = 0.353 \pm 0.014\,. \end{aligned} \tag{3.70}$$

In the SM, the non-vanishing of the $\bar{\eta}$ parameter [related to the phase φ in (3.66) and (3.67)] is the only source of CP violation in the quark sector (we shall see that new sources of CP violation very likely arise from the neutrino sector). Unitarity of the CKM matrix V implies relations of the form $\sum_a V_{ba}V_{ca}^* = \delta_{bc}$.

In most cases these relations do not imply particularly instructive constraints on the Wolfenstein parameters. But when the three terms in the sum are of comparable magnitude, we get interesting information. The three numbers which must add to zero form a closed triangle in the complex plane (unitarity triangle), with sides of comparable length. This is the case for the *t*–*u* triangle shown in Fig. 3.7 (or, what is equivalent to a first approximation, for the *d*–*b* triangle):

$$V_{td}V_{ud}^* + V_{ts}V_{us}^* + V_{tb}V_{ub}^* = 0\,. \tag{3.71}$$

All terms are of order λ^3. For $\eta = 0$, the triangle would flatten down to vanishing area. In fact, the area J of the triangle, of order $J \sim \eta A^2\lambda^6$, is the Jarlskog invariant [251] (its value is independent of the parametrization). In the SM, in the quark sector, all CP violating observables must be proportional to J, hence to the area of the triangle or to η. Its experimental value is $J \sim (3.12 \pm 0.09) \times 10^{-5}$ [355].

Direct and by now very solid evidence for J being non-vanishing was first obtained from the measurements of ϵ and ϵ' in K decay. Additional direct evidence has more recently been collected from experiments on B decays at beauty factories, at the Tevatron and at the LHC (in particular by the LHCb experiment). Very recently searches for CP violation in D decays (negative so far) have been reported by the LHCb experiment [282]. The angles β (the most precisely measured), α, and γ have been determined with fair precision. The angle measurements and the available information on the magnitude of the sides, taken together, are in good agreement with the predictions from the SM unitary triangle (see Fig. 3.8) [344, 355]. Some alleged tensions are not convincing, either because of their poor statistical significance or because of lack of confirmation from different potentially

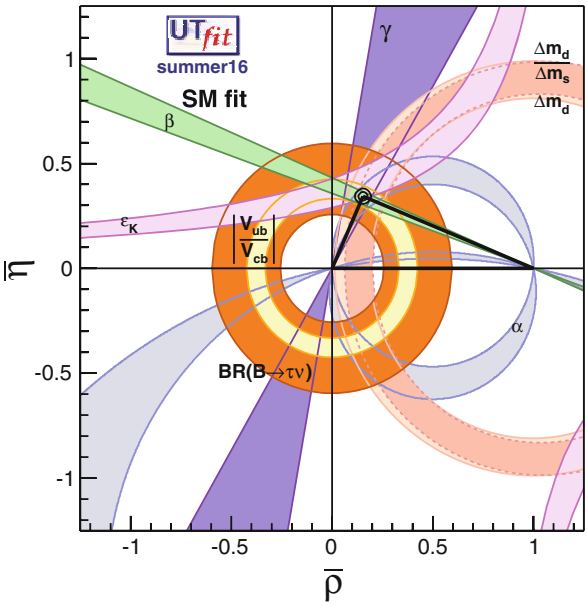

Fig. 3.8 Constraints in the $\bar{\rho}, \bar{\eta}$ plane, including the most recent data inputs in the global CKM fit. From [107] (with permission)

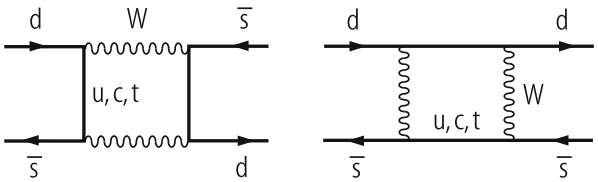

Fig. 3.9 Box diagrams describing K^0–$\bar{K}^0$ mixing at the quark level at 1-loop

sensitive experiments, or because the associated theoretical error estimates can be questioned.

As we have discussed, due to the GIM mechanism, there are no flavour-changing neutral current (FCNC) transitions at the tree level in the SM. Transitions with $|\Delta F| = 1, 2$ are induced at one-loop level. In particular, meson mixing, i.e., $M \to \bar{M}$ off-diagonal $|\Delta F| = 2$ mass matrix elements (with $M = K, D$, or B neutral mesons), are obtained from box diagrams. For example, in the case of K^0–$\bar{K}^0$ mixing, the relevant transition is $\bar{s}d \to s\bar{d}$ (see Fig. 3.9). In the internal quark lines, all up-type quarks are exchanged. In the amplitude, two vertices and the connecting propagator (with virtual four momentum p_μ) at one side contribute a factor ($u_i = u, c, t$):

$$F_{\text{GIM}} = \sum_i V^*_{u_i s} \frac{1}{\not{p} - m_{ui}} V_{u_i d} \,, \tag{3.72}$$

which, in the limit of equal m_{ui}, is clearly vanishing due to the unitarity of the CKM matrix V. Thus the result is proportional to mass differences.

For K^0–$\bar{K}^0$ mixing, the contribution of virtual u quarks is negligible due to the small value of m_u and the contribution of the t quark is also small due to the mixing factors $V_{ts}^* V_{td} \sim O(A^2\lambda^5)$. The dominant c quark contribution to the real part of the box diagram quark-level amplitude is approximately of the form (see, for example, [176]):

$$\mathrm{Re}\, H_{\mathrm{box}} = \frac{G_{\mathrm{F}}^2}{16\pi^2} m_c^2 \mathrm{Re}(V_{cs}^* V_{cd})^2 \eta_1 O^{\Delta s=2} \,, \tag{3.73}$$

where $\eta_1 \sim 0.85$ is a QCD correction factor and $O^{\Delta s=2} = \bar{d}_{\mathrm{L}} \gamma_\mu s_{\mathrm{L}} \bar{s}_{\mathrm{L}} \gamma_\mu d_{\mathrm{L}}$ is the relevant 4-quark dimension-6 operator. The η_1 factor arises from gluon exchanges among the quark legs of the 4-quark operator. Indeed the coefficients of the operator expansion, which arises when the heavy particles exchanged are integrated away, obey renormalization group equations, and the associated logarithms can be resummed. (The first calculation of resummed QCD corrections to weak non-leptonic amplitudes was carried out in [209]. For a pedagogical introduction see, for example, [116].) To obtain the K^0–$\bar{K}^0$ mixing amplitude, the matrix element of $O^{\Delta s=2}$ between meson states must be taken, and this is parametrized by a "B_K parameter", defined in such a way that $B_K = 1$ for vacuum state insertion between the two currents:

$$\left\langle K^0 | O^{\Delta s=2} | \bar{K}^0 \right\rangle = \frac{16}{3} f_K m_K^2 B_K \,, \tag{3.74}$$

where $B_K \sim 0.75$ (this is the renormalization group independent definition, usually denoted by $\hat{B}_K$) and $f_K \sim 113\,\mathrm{MeV}$, the kaon pseudoscalar constant, are best evaluated by QCD lattice simulations [348]. Clearly, additional non-perturbative terms must be added to the charm parton contribution in (3.73), some of them of $O(m_K^2/m_c^2)$, because the smallness of m_c makes a completely partonic dominance inadequate. In (3.73), the factor $O(m_c^2/m_W^2)$ is the "GIM suppression" factor [$1/m_W^2$ is hidden in G_{F} according to (3.16)].

For B mixing the dominant contribution is from the t quark. In this case, the partonic dominance is more realistic and the GIM factor $O(m_t^2/m_W^2)$ is actually larger than 1. More recently D mixing has also been observed [53]. In the corresponding box diagrams, down-type quarks are involved. But starting from $D \sim c\bar{u}$, the b quark contribution is strongly suppressed by the CKM angles, given that $V_{cb} V_{ub}^* \sim O(\lambda_C^5)$. The masses of the d and s quarks are too small for a partonic evaluation of the box diagram, and non-perturbative terms cannot be neglected. This makes a theoretical evaluation of mixing and CP violation effects for D mesons problematic.

All sorts of transitions with $|\Delta F| = 1$ are also induced at loop level. For example, an effective vertex $Z \to t\bar{c}$, which does not exist at tree level, is generated at 1-loop

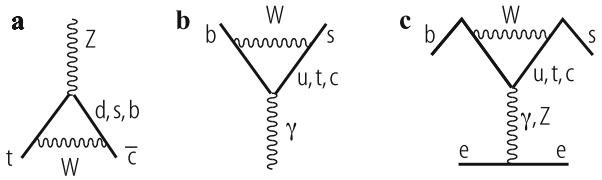

Fig. 3.10 Examples of $|\Delta F| = 1$ transitions at the quark level at 1-loop: (**a**) Diagram for a $Z \to t\bar{c}$ vertex, (**b**) $b \to s\gamma$, and (**c**) a "penguin" diagram for $b \to se^+e^-$

(see Fig. 3.10). Similarly, transitions involving photons or gluons are also possible, like $t \to cg$ or $b \to s\gamma$ (Fig. 3.10), or again $b \to sg$.

For light fermion exchange in the loop, the GIM suppression is also effective in $|\Delta F| = 1$ amplitudes. For example, analogous leptonic transitions like $\mu \to e\gamma$ or $\tau \to \mu\gamma$ also exist, but in the SM are extremely small and out of reach for experiments, because the tiny neutrino masses enter into the GIM suppression factor. But new physics effects could well make these rare lepton flavour-violating processes accessible to experiment. In fact, the present limits already pose stringent constraints on models of new physics. Of particular importance is the recent bound obtained by the MEG Collaboration at SIN, near Zurich, Switzerland, on the branching ratio for $\mu \to e\gamma$, viz., $B(\mu \to e\gamma) \lesssim 5.7 \times 10^{-13}$ at 90% [16].

The external Z, photon, or gluon can be attached to a pair of light fermions, giving rise to an effective four-fermion operator, as in "penguin diagrams" like the one shown in Fig. 3.10 for $b \to sl^+l^-$. The inclusive rate $B \to X_s\gamma$ (here B stands for B_d) with X_s a hadronic state containing a unit of strangeness corresponding to an s quark, has been precisely measured. The world average result for the branching ratio with $E_\gamma > 1.6\,\text{GeV}$ is [53]

$$B(B \to X_s\gamma)_{\text{exp}} = (3.55 \pm 0.26) \times 10^{-4} \,.$$

The theoretical prediction for this inclusive process is to a large extent free of uncertainties from hadronization effects and is accessible to perturbation theory as the b quark is heavy enough. The most complete result to order α_s^2 is at present from [86] (and references therein):

$$B(B \to X_s\gamma)_{\text{th}} = (2.98 \pm 0.26) \times 10^{-4} \,.$$

Note that the theoretical value has recently become smaller than the experimental value. The fair agreement between theory and experiment imposes stringent constraints on possible new physics effects.

Related processes are $B_{s,d} \to \mu^+\mu^-$. These decays are very rare in the SM, their predicted branching ratio being [117]

$$B(B_s \to \mu^+\mu^-) \sim (3.35 \pm 0.28) \times 10^{-9} \,, \quad B(B_d \to \mu^+\mu^-) \sim (1.07 \pm 0.10) \times 10^{-10} \,.$$

These very small expected branching ratios result because these decays are FCNC processes with helicity suppression in the purely leptonic final state (the decaying meson has spin zero and the muon pair is produced by vector exchange in the SM). Many models of new physics beyond the SM predict large deviations. Thus these processes represent very stringent tests of the SM.

Recently, the LHCb and CMS experiments have reached the sensitivity to observe the B_s mode. The LHCb result is [5]

$$B(B_s \to \mu^+\mu^-) = 2.9^{+1.1}_{-1.0} \times 10^{-9} ,$$

and the same paper sets the bound

$$B(B_d \to \mu^+\mu^-) \leq 7.4 \times 10^{-10} \quad \text{at 95\% confidence level} .$$

For the same decays, CMS has obtained [136]

$$B(B_s \to \mu^+\mu^-) = 3.0^{+1.0}_{-0.9} \times 10^{-9} ,$$

and

$$B(B_d \to \mu^+\mu^-) \leq 11 \times 10^{-10} \quad \text{at 95\% confidence level} .$$

The LHCb and CMS results have been combined [352] and give

$$B(B_s \to \mu^+\mu^-) = (2.9 \pm 0.7)^{-9} ,$$

in good agreement with the SM, and

$$B(B_d \to \mu^+\mu^-) = 3.6^{+1.6}_{-1.4} \times 10^{-10} ,$$

with the central value 1.7σ above the SM. Another very demanding test of the SM has been passed!

Among the exclusive processes of the $b \to s$ type, much interest is at present devoted to the channel $B \to K^*\mu^+\mu^-$ [4, 106]. The differential decay distribution depends on three angles and on the $\mu^+\mu^-$ invariant mass squared q^2. In general $12 + 12$ form factors enter into the decay distribution (12 in B decay and 12 in the CP conjugated $\bar{B}$ decay), and many observables can be defined. By suitable angular foldings and CP averages, the number of form factors is reduced. A sophisticated theoretical analysis allows one to identify and study a number of quantities that can be measured and are "clean", i.e., largely independent of hadronic form factor ambiguities [106]. For those observables most of the results agree with the SM predictions (based on a Wilson operator expansion in powers of $1/m_W$ and $1/m_b$, with coefficients depending on α_s), but a few discrepancies are observed. The significance, taking into account the number of observables studied

and the theoretical ambiguities (especially in the estimate of $1/m_b$ corrections), is not compelling, but a substantial activity is under way on both the experimental and the theoretical side (see, for example, [248]). Watch this space!

In conclusion, the CKM theory of quark mixing and CP violation has been precisely tested in the last decade and turns out to be very successful. The expected deviations from new physics at the EW scale have not yet appeared. The constraints on new physics from flavour phenomenology are extremely demanding: when adding higher dimensional effective operators to the SM, the flavour constraints generically lead to powers of very large suppression scales Λ in the denominators of the corresponding coefficients. In fact, in the SM, as we have discussed in this section, there are very powerful protections against flavour-changing neutral currents and CP violation effects, in particular through the smallness of quark mixing angles. In this respect the SM is very special and, as a consequence, if there is new physics, it must be highly non-generic in order to satisfy the present flavour constraints.

Only by requiring new physics to share the SM set of protections can one reduce the scale Λ down to $O(1)$ TeV. For example, the class of models with minimal flavour violation (MFV) [152], where the SM Yukawa couplings are the only flavour symmetry breaking terms also beyond the SM, have been much studied and represent a sort of extreme baseline. Alternative, less minimal models that are currently under study are based on a suitably broken $U(3)^3$ or $U(2)^3$ flavour symmetry (the cube refers to the $Q_{\mathrm{L}} = u_{\mathrm{L}}$, d_{L} doublet and the two u_{R} and d_{R} singlets, while $U(3)$ or $U(2)$ mix the three or the first two generations) [81].

3.7 Neutrino Mass and Mixing

In the minimal version of the SM, the right-handed neutrinos $\nu_{i\mathrm{R}}$, which have no gauge interactions, are not present at all. With no ν_{R}, no Dirac mass is possible for neutrinos. If lepton number conservation is also imposed, then no Majorana mass is allowed either, and as a consequence, all neutrinos are massless. But at present, from neutrino oscillation experiments, we know that at least two out of the three known neutrinos have non-vanishing masses (for reviews, see, for example, [36]): the two mass-squared differences measured from solar (Δm^2_{12}) and atmospheric oscillations (Δm^2_{23}) are given by $\Delta m^2_{12} \sim 8 \times 10^{-5}\,\mathrm{eV}^2$ and $\Delta m^2_{23} \sim 2.5 \times 10^{-3}\,\mathrm{eV}^2$ [200, 201, 229].

Neutrino oscillations only measure $|m_i^2|$ differences. Regarding the absolute values of each m_i we know that they are very small, with an upper limit of a fraction of an eV, obtained from the following:

- Laboratory experiments, e.g., tritium β decay near the end point, which gives $m_\nu \lesssim 2\,\mathrm{eV}$ [307].
- Absence of visible neutrinoless double β decay ($0\nu\beta\beta$). From Ge^{76}, it has been shown that $|m_{ee}| \lesssim 0.2$–$0.4\,\mathrm{eV}$ [21]. The range is from nuclear matrix element

ambiguities and m_{ee} is a combination of neutrino masses (for a review, see, for example, [373]). This result strongly disfavours, in a model-independent way, the claimed observation of $0\nu\beta\beta$ decay in Ge^{76} decays [267]. From Xe^{136}, one obtains the combined result $|m_{ee}| \lesssim 0.12$–$0.25\,\mathrm{eV}$ [69].

- Cosmological observations [175]. After the recent release of the Planck data, the quoted bounds for Σm_ν, the sum of (quasi-)stable neutrino masses, span a range, depending on the data set included and the cosmological priors, like $\Sigma m_\nu \lesssim 0.98$ or $\lesssim 0.32$ or $\lesssim 0.23$ [18] (assuming three degenerate neutrinos, these numbers have to be divided by 3 in order to obtain the limit on individual neutrino masses).

If $\nu_{i\mathrm{R}}$ are added to the minimal model and lepton number is imposed by hand, then neutrino masses would in general appear as Dirac masses, generated by the Higgs mechanism, as for any other fermion. But for Dirac neutrinos, to explain the extreme smallness of neutrino masses, one should allow for very small Yukawa couplings. However, we stress that, in the SM, baryon B and lepton L number conservation, which are not guaranteed by gauge symmetries (although this is the case for the electric charge Q), are understood as "accidental" symmetries. In fact the SM Lagrangian should contain all terms allowed by gauge symmetry and renormalizability, but the most general renormalizable Lagrangian (i.e., with operator dimension $d \leq 4$), built from the SM fields, compatible with the SM gauge symmetry, in the absence of $\nu_{i\mathrm{R}}$, is automatically B and L conserving. (However, non-perturbative instanton effects break the conservation of $B + L$ while preserving $B - L$, as discussed in Sect. 3.8.)

In the presence of $\nu_{i\mathrm{R}}$, this is no longer true, and the right-handed Majorana mass term is allowed:

$$M_{RR} = \bar{\nu}^{\mathrm{c}}_{i\mathrm{R}} M_{ij} \nu_{j\mathrm{R}} = \nu^{\mathrm{T}}_{i\mathrm{R}} C M_{ij} \nu_{j\mathrm{R}} \,, \tag{3.75}$$

where $\nu^{\mathrm{c}}_{i\mathrm{R}} = C\bar{\nu}^{\mathrm{T}}_{i\mathrm{R}}$ is the charge-conjugated neutrino field and C is the charge conjugation matrix in Dirac spinor space. The Majorana mass term is an operator of dimension $d = 3$ with $\Delta L = 2$. Since the $\nu_{i\mathrm{R}}$ are gauge singlets, the Majorana mass M_{RR} is fully allowed by the gauge symmetry and a coupling with the Higgs is not needed to generate this type of mass. As a consequence, the mass matrix entries M_{ij} do not need to be of the order of the EW symmetry breaking scale v, and could be much larger. If one starts from the Dirac and RR Majorana mass terms for neutrinos, the resulting mass matrix, in the L, R space, has the form

$$m_\nu = \begin{bmatrix} 0 & m_{\mathrm{D}} \\ m_{\mathrm{D}} & M \end{bmatrix} \,, \tag{3.76}$$

where m_{D} and M are the Dirac and Majorana mass matrices [M is the matrix M_{ij} in (3.75)]. The corresponding eigenvalues are three very heavy neutrinos with masses of order M and three light neutrinos with masses

$$m_\nu = -m^{\mathrm{T}}_{\mathrm{D}} M^{-1} m_{\mathrm{D}} \,, \tag{3.77}$$

which are possibly very small if M is large enough. This is the see-saw mechanism for neutrino masses [291]. Note that, if no ν_{iR} existed, a Majorana mass term could still be built out of ν_{jL}. But ν_{jL} have weak isospin 1/2, being part of the left-handed lepton doublet l. Thus, the left-handed Majorana mass term has total weak isospin equal to 1 and needs two Higgs fields to make a gauge invariant term. The resulting mass term, viz.,

$$O_5 = \frac{(Hl)_i^{\mathrm{T}} \lambda_{ij} (Hl)_j}{M} + \text{h.c.}, \tag{3.78}$$

with M a large scale (a priori comparable to the scale of M_{RR}) and λ a dimensionless coupling generically of $O(1)$, is a non-renormalizable operator of dimension 5, first pointed out by S. Weinberg [363]. The corresponding mass terms are of the order $m_\nu \sim \lambda v^2/M$, where v is the Higgs VEV, hence of the same generic order as the light neutrino masses from (3.77). Note that, in general, the neutrino mass matrix has the form

$$\mathbf{m}_\nu = \nu^{\mathrm{T}} m_\nu \nu \ , \tag{3.79}$$

as a consequence of the Majorana nature of neutrinos.

In conclusion, neutrino masses are believed to be small because neutrinos are Majorana particles with masses inversely proportional to the large scale M of energy where L non-conservation is induced. This corresponds to an important enlargement of the original minimal SM, where no ν_R was included and L conservation was imposed by hand (but this ansatz would be totally unsatisfactory because L conservation is true "accidentally" only at the renormalizable level, but is violated by non-renormalizable terms like the Weinberg operator and by instanton effects). Actually, L and B non-conservation are necessary if we want to explain baryogenesis and we have Grand Unified Theories (GUTs) in mind. It is interesting that the observed magnitudes of the mass-squared splittings of neutrinos are well compatible with a scale M remarkably close to the GUT scale, where L non-conservation is indeed naturally expected. In fact, for $m_\nu \approx \sqrt{\Delta m^2_{\text{atm}}} \approx 0.05$ eV (see Table 3.1) and $m_\nu \approx m_{\mathrm{D}}^2/M$ with $m_{\mathrm{D}} \approx v \approx 200\,\text{GeV}$, we find $M \approx 10^{15}$ GeV which indeed is an impressive indication for M_{GUT}.

Table 3.1 Fits to neutrino oscillation data from [229] (free fluxes, including short baseline reactor data)

Δm^2_{sun} (10^{-5} eV^2)	$7.45^{+0.19}_{-0.16}$
Δm^2_{atm} (10^{-3} eV^2)	2.417 ± 0.013 (-2.410 ± 0.062)
$\sin^2\theta_{12}$	0.306 ± 0.012
$\sin^2\theta_{23}$	$0.446 \pm 0.007 \bigoplus 0.587^{+0.032}_{-0.037}$
$\sin^2\theta_{13}$	$0.0229^{+0.0020}_{-0.0019}$
δ_{CP} (°)	265^{+56}_{-61}

The results for both the normal and the inverse (in brackets) hierarchies are shown

In the previous section, we discussed flavour mixing for quarks. But clearly, given that non-vanishing neutrino masses have been established, a similar mixing matrix is also introduced in the leptonic sector. We assume in the following that there are only two distinct neutrino oscillation frequencies, the atmospheric and the solar frequencies (both of them now also confirmed by experiments where neutrinos are generated on the Earth like K2K, KamLAND, and MINOS). At present the bulk of neutrino oscillation data are well reproduced in terms of three light neutrino species. However, some (so far not compelling) evidence for additional "sterile" neutrino species (i.e., not coupled to the weak interactions, as demanded by the LEP limit on the number of "active" neutrinos) are present in some data. We discuss here 3-neutrino mixing, which is in any case a good approximate framework to discuss neutrino oscillations, while for possible sterile neutrinos we refer to the comprehensive review in [8].

Neutrino oscillations are due to a misalignment between the flavour basis, i.e., $\nu' \equiv (\nu_e, \nu_\mu, \nu_\tau)$, where ν_e is the partner of the mass and flavour eigenstate e^- in a left-handed (LH) weak isospin $SU(2)$ doublet (similarly for ν_μ and ν_τ)) and the mass eigenstates $\nu \equiv (\nu_1, \nu_2, \nu_3)$ [36, 280, 312]:

$$\nu' = U\nu \ , \tag{3.80}$$

where U is the unitary $\times 3$ mixing matrix. Given the definition of U and the transformation properties of the effective light neutrino mass matrix $\mathbf{m_\nu}$ in (3.79), viz.,

$$\nu'^{\mathrm{T}} m_\nu \nu' = \nu^{\mathrm{T}} U^{\mathrm{T}} m_\nu U \nu \ , \qquad U^{\mathrm{T}} m_\nu U = \mathrm{Diag}\,(m_1, m_2, m_3) \equiv m_{\mathrm{diag}} \ , \tag{3.81}$$

we obtain the general form of m_ν (i.e., of the light ν mass matrix in the basis where the charged lepton mass is a diagonal matrix):

$$m_\nu = U^* m_{\mathrm{diag}} U^\dagger \ . \tag{3.82}$$

The matrix U can be parameterized in terms of three mixing angles θ_{12}, θ_{23}, and θ_{13} ($0 \le \theta_{ij} \le \pi/2$) and one phase φ ($0 \le \varphi \le 2\pi$) [122], exactly as for the quark mixing matrix V_{CKM}. The following definition of mixing angles can be adopted:

$$U = \begin{pmatrix} 1 & 0 & 0 \\ 0 & c_{23} & s_{23} \\ 0 & -s_{23} & c_{23} \end{pmatrix} \begin{pmatrix} c_{13} & 0 & s_{13}\mathrm{e}^{\mathrm{i}\varphi} \\ 0 & 1 & 0 \\ -s_{13}\mathrm{e}^{-\mathrm{i}\varphi} & 0 & c_{13} \end{pmatrix} \begin{pmatrix} c_{12} & s_{12} & 0 \\ -s_{12} & c_{12} & 0 \\ 0 & 0 & 1 \end{pmatrix} \ , \tag{3.83}$$

where $s_{ij} \equiv \sin\theta_{ij}$ and $c_{ij} \equiv \cos\theta_{ij}$. In addition, if ν are Majorana particles, we have two more phases [101] given by the relative phases among the Majorana masses m_1, m_2, and m_3. If we choose m_3 real and positive, these phases are carried by $m_{1,2} \equiv |m_{1,2}|\mathrm{e}^{\mathrm{i}\phi_{1,2}}$. Thus, in general, nine parameters are added to the SM when non-vanishing neutrino masses are included: three eigenvalues, three mixing angles, and three CP violating phases.

In our notation the two frequencies, $\Delta m_I^2/4E$ (I = sun, atm), are parametrized in terms of the ν mass eigenvalues by

$$\Delta m^2_{\rm sun} \equiv |\Delta m^2_{12}|\,, \qquad \Delta m^2_{\rm atm} \equiv |\Delta m^2_{23}|\,. \tag{3.84}$$

where $\Delta m^2_{12} = |m_2|^2 - |m_1|^2 > 0$ and $\Delta m^2_{23} = m_3^2 - |m_2|^2$. The numbering 1,2,3 corresponds to a definition of the frequencies and in principle may not coincide with the ordering from the lightest to the heaviest state. "Normal hierarchy" is the case where m_3 is the largest mass in absolute value, otherwise one has an "inverse hierarchy".

Very important developments occurred in the data in 2012. The value of the mixing angle θ_{13} was shown to be non-vanishing and its value is now known to fair accuracy. Several experiments were involved in the θ_{13} measurement and their results are reported in Fig. 3.11. The most precise result is from the Daya Bay reactor experiment in China:

$$\sin^2 2\theta_{13} = 0.090 \pm 0.012\,,\ \text{or}\ \sin^2\theta_{13} = 0.023 \pm 0.003\,,\ \text{or}\ \theta_{13} \sim 0.152 \pm 0.010\,. \tag{3.85}$$

Note that θ_{13} is somewhat smaller but of the same order as the Cabibbo angle $\theta_{\rm C}$. The present data on the oscillation parameters are summarized in Table 3.1 [229].

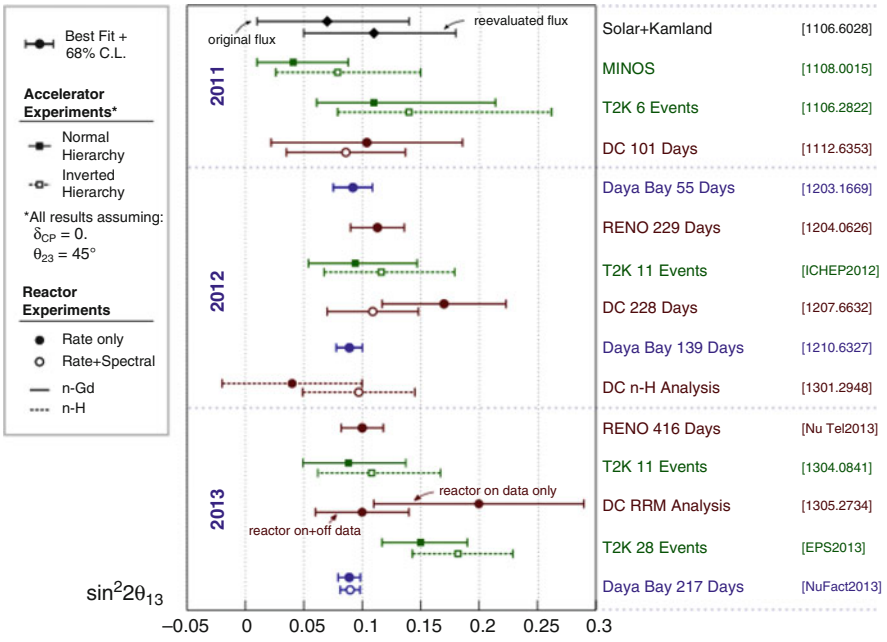

Fig. 3.11 Reactor angle measurements, updated to the NUFACT13 Conference, August 2013 [259], from the experiments T2K [12], MINOS [17], DOUBLE CHOOZ [13], Daya Bay [54], and RENO [23], for the normal (inverse) hierarchy. Figure credit: S. Jetter

Neutrino mixing is important because it could in principle provide new clues for the understanding of the flavour problem. Even more so since neutrino mixing angles show a pattern that is completely different from that of quark mixing: for quarks all mixing angles are small, while for neutrinos two angles are large (one is still compatible with the maximal value) and only the third one is small. In reality, it is frustrating that there has been no real illumination of the problem of flavour. Models can reproduce the data on neutrino mixing in a wide range of dynamical setups that goes from anarchy to discrete flavour symmetries (for reviews and references see, for example, [35, 37, 50–52, 264]), but we have not yet been able to single out a unique and convincing baseline for the understanding of fermion masses and mixings. Despite many interesting ideas and the formulation of many elegant models, the mysteries of the flavour structure of the three generations of fermions have not yet been unveiled.

3.8 Quantization and Renormalization of the Electroweak Theory

The Higgs mechanism gives masses to the Z, the $W^{\pm}$, and to fermions, while the Lagrangian density is still symmetric. In particular the gauge Ward identities and the symmetric form of the gauge currents are preserved. The validity of these relations is an essential ingredient for renormalizability. In the previous sections, we have specified the Feynman vertices in the "unitary" gauge, where only physical particles appear. However, as discussed in Chap. 1, in this gauge the massive gauge boson propagator would have a bad ultraviolet behaviour:

$$W_{\mu\nu} = \frac{-g_{\mu\nu} + q_\mu q_\nu / m_W^2}{q^2 - m_W^2} \,. \tag{3.86}$$

A formulation of the standard EW theory with good apparent ultraviolet behaviour can be obtained by introducing the renormalizable or R_ξ gauges [14], in analogy with the Abelian case discussed in detail in Chap. 1. One parametrizes the Higgs doublet as

$$\phi = \begin{pmatrix} \phi^+ \\ \phi^0 \end{pmatrix} = \begin{pmatrix} \phi_1 + \mathrm{i}\phi_2 \\ \phi_3 + \mathrm{i}\phi_4 \end{pmatrix} = \begin{pmatrix} -\mathrm{i}w^+ \\ v + (H + \mathrm{i}z)/\sqrt{2} \end{pmatrix} \,, \tag{3.87}$$

and similarly for $\phi^\dagger$, where w^- appears. The scalar fields $w^{\pm}$ and z are the pseudo-Goldstone bosons associated with the longitudinal modes of the physical vector bosons $W^{\pm}$ and Z. The R_ξ gauge fixing Lagrangian has the form

$$\Delta\mathscr{L}_{\mathrm{GF}} = -\frac{1}{\xi}\left|\partial^\mu W_\mu - \xi m_W w\right|^2 - \frac{1}{2\eta}(\partial^\mu Z_\mu - \eta m_Z z)^2 - \frac{1}{2\alpha}(\partial^\mu A_\mu)^2 \,. \tag{3.88}$$

The $W^{\pm}$ and Z propagators, as well as those of the scalars $w^{\pm}$ and z, have exactly the same general forms as for the Abelian case in (1.67)–(1.69), with parameters ξ and η, respectively (and the pseudo-Goldstone bosons $w^{\pm}$ and z have masses ξm_W and ηm_Z). In general, a set of associated ghost fields must be added, again in direct analogy with the treatment of R_ξ gauges in the Abelian case of Chap. 1. The complete Feynman rules for the standard EW theory can be found in a number of textbooks (see, for example, [137]).

The pseudo-Goldstone bosons $w^{\pm}$ and z are directly related to the longitudinal helicity states of the corresponding massive vector bosons $W^{\pm}$ and Z. This correspondence materializes in a very interesting "equivalence theorem": at high energies of order E, the amplitude for the emission of one or more longitudinal gauge bosons $V_{\rm L}$ (with $V = W, Z$) becomes equal (apart from terms reduced by powers of m_V/E) to the amplitude where each longitudinal gauge boson is replaced by the corresponding Goldstone field $w^{\pm}$ or z [149]. For example, consider top decay with a longitudinal W in the final state: $t \to bW^+_{\rm L}$. The equivalence theorem asserts that we can compute the dominant contribution to this rate from the simpler $t \to bw^+$ matrix element:

$$\Gamma(t \to bW^+_{\rm L}) = \Gamma(t \to bw^+)\left[1 + O(m_W^2/m_t^2)\right] . \tag{3.89}$$

In fact, one finds

$$\Gamma(t \to bw^+) = \frac{h_t^2}{32\pi} m_t = \frac{G_{\rm F} m_t^3}{8\pi\sqrt{2}} , \tag{3.90}$$

where $h_t = m_t/v$ is the Yukawa coupling of the top quark (numerically very close to 1), and we used $1/v^2 = 2\sqrt{2}G_{\rm F}$ [see (3.51)]. If we compare with (3.31), we see that this expression coincides with the total top width (i.e., including all polarizations for the W in the final state), computed at tree level, apart from terms reduced by powers of $O(m_W^2/m_t^2)$. In fact, the longitudinal W is dominant in the final state because $h_t^2 \gg g^2$. Similarly, the equivalence theorem can be applied to find the dominant terms at large $\sqrt{s}$ for the cross-section $e^+e^- \to W^+_{\rm L} W^-_{\rm L}$, or the leading contribution, in the limit $m_{\rm H} \gg m_V$, to the width for the decay $\Gamma(H \to VV)$.

The formalism of the R_ξ gauges is also very useful in proving that spontaneously broken gauge theories are renormalizable. In fact, the non-singular behaviour of propagators at large momenta is very suggestive of the result. Nevertheless, it is not at all a simple matter to prove this statement. The fundamental theorem that a gauge theory with spontaneous symmetry breaking and the Higgs mechanism is in general renormalizable was proven by 't Hooft and Veltman [278, 358].

For a chiral theory like the SM an additional complication arises from the existence of chiral anomalies. But this problem is avoided in the SM because the quantum numbers of the quarks and leptons in each generation imply a remarkable (and, from the point of view of the SM, mysterious) cancellation of the anomaly, as originally observed in [109]. In quantum field theory, one encounters an

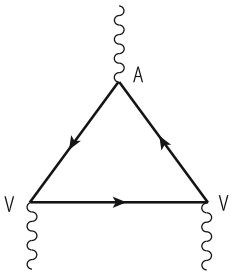

Fig. 3.12 Triangle diagram that generates the ABJ anomaly [19]

anomaly when a symmetry of the classical Lagrangian is broken by the process of quantization, regularization, and renormalization of the theory. Of direct relevance for the EW theory is the Adler–Bell–Jackiw (ABJ) chiral anomaly [19]. The classical Lagrangian of a theory with massless fermions is invariant under $U(1)$ chiral transformations $\psi\prime = \mathrm{e}^{\mathrm{i}\gamma_5\theta}\psi$ (see also Sect. 2.2.3). The associated axial Noether current is conserved at the classical level. But at the quantum level, chiral symmetry is broken due to the ABJ anomaly and the current is not conserved. The chiral breaking is produced by a clash between chiral symmetry, gauge invariance, and the regularization procedure.

The anomaly is generated by triangular fermion loops with one axial and two vector vertices (Fig. 3.12). For example, for the Z, the axial coupling is proportional to the third component of weak isospin t_3, while the vector coupling is proportional to a linear combination of t_3 and the electric charge Q. Thus in order for the chiral anomaly to vanish, all traces of the form $\mathrm{tr}\{t_3QQ\}$, $\mathrm{tr}\{t_3t_3Q\}$, $\mathrm{tr}\{t_3t_3t_3\}$ (and also $\mathrm{tr}\{t_+t_-t_3\}$ when charged currents are included) must vanish, where the trace is extended over all fermions in the theory that can circulate in the loop. Now all of these traces happen to vanish for each fermion family separately. For example, take $\mathrm{tr}\{t_3QQ\}$. In one family there are, with $t_3 = +1/2$, three colours of up quarks with charge $Q = +2/3$ and one neutrino with $Q = 0$ and, with $t_3 = -1/2$, three colours of down quarks with charge $Q = -1/3$ and one l^- with $Q = -1$. Thus we obtain

$$\mathrm{tr}\{t_3QQ\} = \frac{1}{2}\times 3\times\frac{4}{9} - \frac{1}{2}\times 3\times\frac{1}{9} - \frac{1}{2}\times 1 = 0\ .$$

This impressive cancellation suggests an interplay among weak isospin, charge, and colour quantum numbers, which appears as a miracle from the point of view of the low energy theory, but is in fact understandable from the point of view of the high energy theory. For example, in Grand Unified Theories (GUTs) (for reviews, see, for example, [315]) there are similar relations where charge quantization and colour are related: in the 5 of $SU(5)$, we have the content $(d, d, d, e^+, \bar{\nu})$ and the charge generator has a vanishing trace in each $SU(5)$ representation: the condition of unit determinant, represented by the letter S in the $SU(5)$ group name, translates into zero trace for the generators. Thus the charge of d quarks is $-1/3$ of the positron charge, because there are three colours. A whole family fits perfectly in one 16 dimensional

representation of $SO(10)$ which is anomaly free. So GUTs can naturally explain the cancellation of the chiral anomaly.

An important implication of chiral anomalies together with the topological properties of the vacuum in non-Abelian gauge theories is that the conservation of the charges associated with baryon (B) and lepton (L) numbers is broken by the anomaly [336], so that B and L conservation are actually violated in the standard electroweak theory (but $B - L$ remains conserved). B and L are conserved to all orders in the perturbative expansion, but the violation occurs via non-perturbative instanton effects [87] [The amplitude is proportional to the typical non-perturbative factor $\exp(-c/g^2)$, with c a constant and g the $SU(2)$ gauge coupling.] The corresponding effect is totally negligible at zero temperature T, but becomes relevant at temperatures close to the electroweak symmetry breaking scale, precisely at $T \sim O(\text{TeV})$. The non-conservation of $B + L$ and the conservation of $B - L$ near the weak scale plays a role in the theory of baryogenesis that aims quantitatively at explaining the observed matter–antimatter asymmetry in the Universe (for reviews and references, see, for example, [115]).

3.9 QED Tests: Lepton Anomalous Magnetic Moments

The most precise tests of the electroweak theory apply to the QED sector. Here we discuss the anomalous magnetic moments of the electron and the muon that are among the most precise measurements in the whole of physics. The magnetic moment μ and the spin $\mathbf{S}$ are related by $\mu = -ge\mathbf{S}/2m$, where g is the gyromagnetic ratio ($g = 2$ for a pointlike Dirac particle). The quantity $a = (g-2)/2$ measures the anomalous magnetic moment of the particle. Recently there have been new precise measurements of a_e and a_μ for the electron [242] and the muon [297]:

$$a_e^{\text{exp}} = 11\,596\,521\,807.3(2.8) \times 10^{-13}\,, \quad a_\mu^{\text{exp}} = 11\,659\,208.9(6.3) \times 10^{-10}\,. \tag{3.91}$$

The theoretical calculations in general contain a pure QED part plus the sum of hadronic and weak contribution terms:

$$a = a^{\text{QED}} + a^{\text{hadronic}} + a^{\text{weak}} = \sum_i C_i \left(\frac{\alpha}{\pi}\right)^i + a^{\text{hadronic}} + a^{\text{weak}}\,. \tag{3.92}$$

The QED part has been computed analytically for $i = 1, 2, 3$, while for $i = 4$ there is a numerical calculation with an error (see, for example, [266] and references therein). The complete numerical evaluation of $i = 5$ for the muon case was published in 2012 [59] as a new and impressive achievement by Kinoshita and his group. The hadronic contribution is from vacuum polarization insertions and from light-by-light scattering diagrams (see Fig. 3.13). The weak contribution is from W or Z exchange.

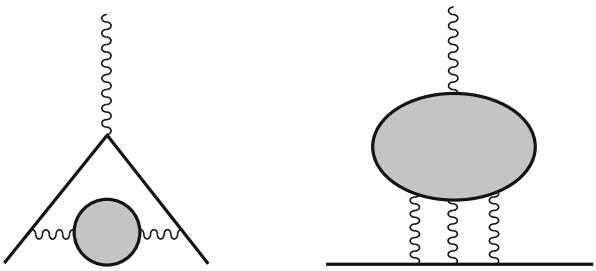

Fig. 3.13 Hadronic contributions to the anomalous magnetic moment: vacuum polarization (*left*) and light-by-light scattering (*right*)

For the electron case, the weak contribution is essentially negligible and the hadronic term $a_e^{\text{hadronic}} \sim (16.82 \pm 0.19) \times 10^{-13}$ does not introduce an important uncertainty. As a result this measurement can be used to obtain the most precise determination of the fine structure constant [59]:

$$\alpha^{-1} \sim 137.035\,999\,165\,7(340)\,, \tag{3.93}$$

In the muon case the experimental precision is less by about three orders of magnitude, but the sensitivity to new physics effects is typically increased by a factor $(m_\mu/m_e)^2 \sim 4 \times 10^4$. One mass factor arises because the effective operator needs a chirality flip and the second because, by definition, one must factor out the Bohr magneton $e/2m$. From the theory side, the QED term, using the value of α from a_e in (3.93), and the weak contribution [151] are affected by small errors and are given by

$$a_\mu^{\text{QED}} = (116\,584\,718.853 \pm 0.037) \times 10^{-11}\,, \quad a_\mu^{\text{weak}} = (154 \pm 2.0) \times 10^{-11}\,, \tag{3.94}$$

where all theoretical numbers are taken from [59].

The dominant ambiguities arise from the hadronic term. The lowest order (LO) vacuum polarization contribution can be evaluated from the measured cross-sections in $e^+e^- \to$ hadrons at low energy via dispersion relations (the largest contribution is from the $\pi\pi$ final state) [155, 239], with the result $a_\mu^{\text{LO}} \times 10^{-11} = 6949 \pm 43$. The higher order (HO) vacuum polarization contribution (from 2-loop diagrams containing a hadronic insertion) is given by $a_\mu^{\text{HO}} \times 10^{-11} = -98.4 \pm 0.7$ [239]. The contribution of the light-by-light (LbL) scattering diagrams is estimated to be $a_\mu^{\text{LBL}} \times 10^{-11} = 116 \pm 40$ [290]. Adding the above contributions, the total hadronic result is reported as

$$a_\mu^{\text{hadronic}} = (6967 \pm 59) \times 10^{-11}\,. \tag{3.95}$$

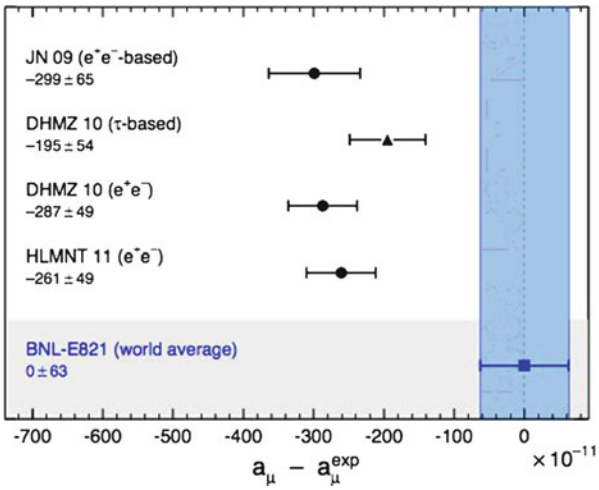

Fig. 3.14 Compilation of recently published results for a_μ (in units of 10^{-11}) [245]: JN [252], DHMZ [155], HLMNT [239]. Figure reproduced with permission. Copyright (c) 2012 by American Physical Society

At face value, this would lead to a 2.9σ deviation from the experimental value $a_\mu^{\rm exp}$ in (3.91):

$$a_\mu^{\rm exp} - a_\mu^{{\rm th}(e^+e^-)} = (249 \pm 87) \times 10^{-11}\,. \tag{3.96}$$

For a recent exchange on the significance of the discrepancy, see [88]. However, the error estimate in the LBL term, mainly a theoretical uncertainty, is not compelling, and it could well be somewhat larger (although probably not by so much as to make the discrepancy completely disappear). A minor puzzle is the fact that, using the conservation of the vector current (CVC) and isospin invariance, which are well established tools at low energy, $a_\mu^{\rm LO}$ can also be evaluated from τ decays. But the results on the hadronic contribution from e^+e^- and from τ decay, nominally of comparable accuracy, are still somewhat different (although the two are now closer than in the past), and the $g-2$ discrepancy would be attenuated if one took the τ result (see Fig. 3.14, which refers to the most recent results). Since it is difficult to find a theoretical reason for the e^+e^- vs τ difference, one must conclude that there is something which is not understood either in the data or in the assessment of theoretical errors. The prevailing view is to take the e^+e^- determination as the most directly reliable, which leads to (3.96), but some doubts remain. Finally, we note that, given the great accuracy of the a_μ measurement and the relative importance of the non-QED contributions, it is not unreasonable that a first signal of new physics would appear in this quantity.

3.10 Large Radiative Corrections to Electroweak Processes

Since the SM theory is renormalizable, higher order perturbative corrections can be reliably computed. Radiative corrections are very important for precision EW tests. The SM inherits all the successes of the old $V-A$ theory of charged currents and QED. Modern tests have focussed on neutral current processes, the W mass, and the measurement of triple gauge vertices. For Z physics and the W mass, the state-of-the-art computation of radiative corrections include the complete one-loop diagrams and selected dominant multi-loop corrections. In addition, some resummation techniques are also implemented, like Dyson resummation of vacuum polarization functions and important renormalization group improvements for large QED and QCD logarithms. We now discuss in more detail sets of large radiative corrections which are particularly significant (for reviews of radiative corrections for LEP1 physics, see, for example, [47], and for a more pedagogical description of LEP physics, see [338]).

Even leaving aside QCD corrections, an important set of quantitative contributions to the radiative corrections arise from large logarithms, e.g., terms of the form

$$\left(\frac{\alpha}{\pi}\ln\frac{m_Z}{m_{f_{ll}}}\right)^n ,$$

where f_{ll} is a light fermion. The sequences of leading and close-to-leading logarithms are fixed by well-known and consolidated techniques (β functions, anomalous dimensions, penguin-like diagrams, etc.). For example, large logarithms from pure QED effects dominate the running of α from m_e, the electron mass, up to m_Z. Similarly, large logarithms of the form

$$\left(\frac{\alpha}{\pi}\ln\frac{m_Z}{\mu}\right)^n$$

also enter, for example, in the relation between $\sin^2\theta_{\rm W}$ at the scales m_Z (LEP, SLC) and μ, e.g., the scale of low-energy neutral-current experiments. Furthermore, large logs from initial state radiation dramatically distort the line shape of the Z resonance, as observed at LEP1 and SLC, and this effect was accurately taken into account for the measurement of the Z mass and total width. The experimental accuracy on m_Z obtained at LEP1 is $\delta m_Z = \pm 2.1$ MeV.

Similarly, a measurement of the total width to an accuracy $\delta\Gamma = \pm 2.3$ MeV has been achieved. The prediction of the Z line shape in the SM to such an accuracy posed a formidable challenge to theory, and it has been successfully met. For the inclusive process $e^+e^- \to f\bar{f}X$, with $f \neq e$ (for a concise discussion, we leave Bhabha scattering aside) and X including photons and gluons, the physical cross-section can be written in the form of a convolution [47]:

$$\sigma(s) = \int_{z_0}^{1} {\rm d}z\, \hat{\sigma}(zs) G(z,s) , \tag{3.97}$$

where $\hat{\sigma}$ is the reduced cross-section, $G(z,s)$ is the radiator function, which describes the effect of initial-state radiation, and $\hat{\sigma}$ includes the purely weak corrections, the effect of final-state radiation (of both photons and gluons), and also non-factorizable terms (initial- and final-state radiation interferences, boxes, etc.) which, being small, can be treated in lowest order and effectively absorbed in a modified $\hat{\sigma}$. The radiator function $G(z,s)$ has an expansion of the form

$$G(z,s) = \delta(1-z) + \frac{\alpha}{\pi}(a_{11}L + a_{10}) + \left(\frac{\alpha}{\pi}\right)^2 (a_{22}L^2 + a_{11}L + a_{20}) + \cdots + \left(\frac{\alpha}{\pi}\right)^n \sum_{i=0}^{n} a_{ni}L^i \,, \tag{3.98}$$

where $L = \ln(s/m_e^2) \simeq 24.2$ for $\sqrt{s} \simeq m_Z$. All first- and second-order terms are known exactly. The sequence of leading and next-to-leading logs can be exponentiated (closely following the formalism of structure functions in QCD). For $m_Z \approx 91\,\text{GeV}$, the convolution displaces the peak by $+110\,\text{MeV}$, and reduces it by a factor of about 0.74. The exponentiation is important in that it amounts to an additional shift of about 14 MeV in the peak position with respect to the 1-loop radiative correction.

Among the one-loop EW radiative corrections, a remarkable class of contributions are those terms that increase quadratically with the top mass. The sensitivity of radiative corrections to m_t arises from the existence of these terms. The quadratic dependence on m_t (and on other possible widely broken isospin multiplets from new physics) arises because, in spontaneously broken gauge theories, heavy virtual particles do not decouple. On the contrary, in QED or QCD, the running of α and α_s at a scale Q is not affected by heavy quarks with mass $M \gg Q$. According to an intuitive decoupling theorem [60], diagrams with heavy virtual particles of mass M can be ignored at $Q \ll M$, provided that the couplings do not grow with M and that the theory with no heavy particles is still renormalizable. In the spontaneously broken EW gauge theories, both requirements are violated.

First, one important difference with respect to unbroken gauge theories is in the longitudinal modes of weak gauge bosons. These modes are generated by the Higgs mechanism, and their couplings grow with masses (as is also the case for the physical Higgs couplings). Second, the theory without the top quark is no longer renormalizable since the gauge symmetry is broken because the (t,b) doublet would not be complete (also the chiral anomaly would not be completely cancelled). With the observed value of m_t, the quantitative importance of the terms of order $G_F m_t^2/4\pi^2\sqrt{2}$ is substantial but not dominant (they are enhanced by a factor $m_t^2/m_W^2 \sim 5$ with respect to ordinary terms). Both the large logarithms and the $G_F m_t^2$ terms have a simple structure and are to a large extent universal, i.e., common to a wide class of processes. In particular, the $G_F m_t^2$ terms appear in vacuum polarization diagrams which are universal (virtual loops inserted in gauge boson internal lines are independent of the nature of the vertices on each side of the propagator) and in the $Z \to b\bar{b}$ vertex which is not. This vertex is specifically sensitive to the top

quark which, being the partner of the b quark in a doublet, runs in the loop. Instead, all types of heavy particles could in principle contribute to vacuum polarization diagrams. The study of universal vacuum polarization contributions, also called "oblique" corrections, and of top enhanced terms is important for an understanding of the pattern of radiative corrections. More generally, the important consequence of non-decoupling is that precision tests of the electroweak theory may a priori be sensitive to new physics, even if the new particles are too heavy for their direct production, but a posteriori no signal of deviation has clearly emerged.

While radiative corrections are quite sensitive to the top mass, they are unfortunately much less dependent on the Higgs mass. In fact, the dependence of one-loop diagrams on $m_{\rm H}$ is only logarithmic, viz., $\sim G_{\rm F} m_W^2 \log(m_H^2/m_W^2)$. Quadratic terms $\sim G_F^2 m_H^2$ only appear at two-loop level [356] and are too small to be detectable. The difference with the top case is that the splitting $m_t^2 - m_b^2$ is a direct breaking of the gauge symmetry that already affects the 1-loop corrections, while the Higgs couplings are "custodial" $SU(2)$ symmetric in lowest order.

3.11 Electroweak Precision Tests

For the analysis of electroweak data in the SM, one starts from the input parameters: as is the case in any renormalizable theory, masses and couplings have to be specified from outside. One can trade one parameter for another and this freedom is used to select the best measured ones as input parameters. Some of them, α, $G_{\rm F}$, and m_Z, are very precisely known, as we have seen, and some others, $m_{f_{\rm light}}$, m_t, and $\alpha_{\rm s}(m_Z)$ are less well determined, while $m_{\rm H}$ was largely unknown before the LHC. In this section we discuss the EW fit without the new input on $m_{\rm H}$ from the LHC, in order to compare the limits so derived on $m_{\rm H}$ with the LHC data. The LHC results will be discussed in the following sections. Among the light fermions, the quark masses are poorly known, but fortunately, for the calculation of radiative corrections, they can be replaced by $\alpha(m_Z)$, the value of the QED running coupling at the Z mass scale. The value of the hadronic contribution to the running, embodied in the value of $\Delta\alpha^{(5)}_{\rm had}(m_Z^2)$ (see Fig. 3.15 [350]) is obtained through dispersion relations from the data on $e^+e^- \to$ hadrons at moderate centre-of-mass energies. From the input parameters, one computes the radiative corrections to a sufficient accuracy to match the experimental accuracy. One then compares the theoretical predictions with the data for the numerous observables which have been measured [351], checks the consistency of the theory, and derives constraints on m_t, $\alpha_{\rm s}(m_Z)$, and $m_{\rm H}$.

The basic tree level relations

$$\frac{g^2}{8m_W^2} = \frac{G_{\rm F}}{\sqrt{2}}\,, \quad g^2 \sin^2\theta_{\rm W} = e^2 = 4\pi\alpha\,, \tag{3.99}$$

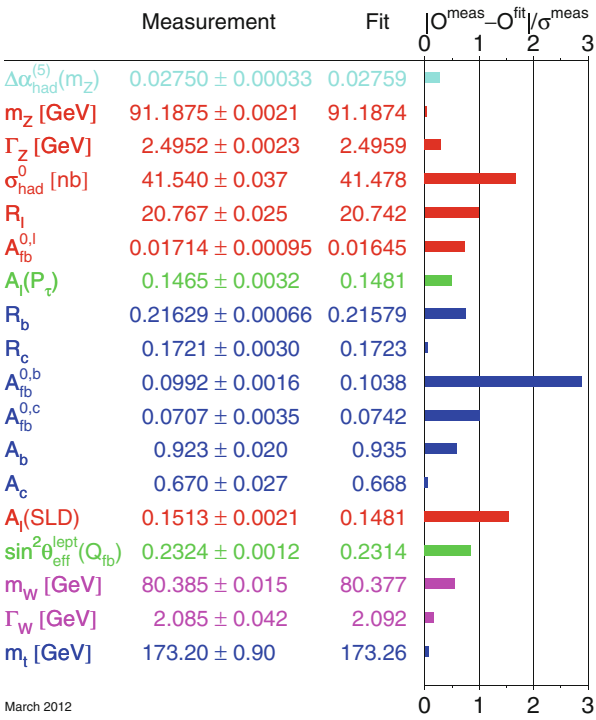

Fig. 3.15 Summary of electroweak precision measurements at high Q^2 [350]. The *first block* shows the Z-pole measurements. The *second block* shows additional results from other experiments: the mass and the width of the W boson measured at the Tevatron and at LEP2, the mass of the top quark measured at the Tevatron, and the contribution to α of the hadronic vacuum polarization. The SM fit results are also shown with the corresponding pulls (differences data and fits in units of standard deviations)

can be combined into

$$\sin^2\theta_{\mathrm{W}} = \frac{\pi\alpha}{\sqrt{2}G_{\mathrm{F}}m_W^2}\,. \tag{3.100}$$

Still at tree level, a different definition of $\sin^2\theta_{\mathrm{W}}$ comes from the gauge boson masses

$$\frac{m_W^2}{m_Z^2\cos^2\theta_{\mathrm{W}}} = \rho_0 = 1 \quad\Longrightarrow\quad \sin^2\theta_{\mathrm{W}} = 1 - \frac{m_W^2}{m_Z^2}\,, \tag{3.101}$$

where $\rho_0 = 1$, assuming that there are only Higgs doublets. The last two relations can be put into the convenient form

$$\left(1 - \frac{m_W^2}{m_Z^2}\right)\frac{m_W^2}{m_Z^2} = \frac{\pi\alpha}{\sqrt{2}G_{\mathrm{F}}m_Z^2}\,. \tag{3.102}$$

Beyond tree level, these relations are modified by radiative corrections:

$$\left(1-\frac{m_W^2}{m_Z^2}\right)\frac{m_W^2}{m_Z^2}=\frac{\pi\alpha(m_Z)}{\sqrt{2}G_{\rm F}m_Z^2}\frac{1}{1-\Delta r_W}\,,$$
$$\frac{m_W^2}{m_Z^2\cos^2\theta_{\rm W}}=1+\Delta\rho_m\,. \tag{3.103}$$

The Z and W masses are to be precisely defined, for example, in terms of the pole position in the respective propagators. Then in the first relation, the replacement of α with the running coupling at the Z mass $\alpha(m_Z)$ makes Δr_W completely determined at 1-loop by purely weak corrections ($G_{\rm F}$ is protected from logarithmic running as an indirect consequence of $V-A$ current conservation in the massless theory). This relation defines Δr_W unambiguously, once the meaning of $m_{W,Z}$ and $\alpha(m_Z)$ is specified (for example, $\bar{M}\bar{S}$). In contrast, in the second relation, $\Delta\rho_m$ depends on the definition of $\sin^2\theta_{\rm W}$ beyond the tree level. For LEP physics $\sin^2\theta_{\rm W}$ is usually defined from the $Z\to\mu^+\mu^-$ effective vertex. At the tree level, the vector and axial-vector couplings $g_{\rm V}^\mu$ and $g_{\rm A}^\mu$ are given in (3.26). Beyond the tree level a corrected vertex can be written down in terms of modified effective couplings. Then $\sin^2\theta_{\rm W}\equiv\sin^2\theta_{\rm eff}$ is generally defined through the muon vertex:

$$\frac{g_{\rm V}^\mu}{g_{\rm A}^\mu}=1\text{–}4\sin^2\theta_{\rm eff}\,,\quad \sin^2\theta_{\rm eff}=(1+\Delta k)s_0^2\,,\quad s_0^2c_0^2=\frac{\pi\alpha(m_Z)}{\sqrt{2}G_{\rm F}m_Z^2}\,,\quad g_{\rm A}^{\mu 2}=\frac{1}{4}(1+\Delta\rho)\,. \tag{3.104}$$

We see that s_0^2 and c_0^2 are "improved" Born approximations (by including the running of α) for $\sin^2\theta_{\rm eff}$ and $\cos^2\theta_{\rm eff}$. Actually, since lepton universality is only broken by masses in the SM, and is in agreement with experiment within the present accuracy, the muon channel can in practice be replaced with the average over charged leptons.

We can write a symbolic equation that summarizes the status of what has been computed up to now for the radiative corrections Δr_W [70], $\Delta\rho$ [193], and Δk [71] (listing some recent work on each item from which older references can be retrieved):

$$\Delta r_W,\Delta\rho,\Delta k=g^2(1+\alpha_{\rm s})+g^2\frac{m_t^2}{m_W^2}(\alpha_s^2+\alpha_s^3)+g^4+g^4\frac{m_t^4}{m_W^4}\alpha_{\rm s}+g^6\frac{m_t^6}{m_W^6}+\cdots\,. \tag{3.105}$$

The meaning of this relation is that the one loop terms of order g^2 are completely known, together with their first order QCD corrections, while the second and third order QCD corrections are only known for the g^2 terms enhanced by m_t^2/m_W^2, the two-loop terms of order g^4 are completely known, and for $\Delta\rho$ alone, the terms $g^4\alpha_{\rm s}$ enhanced by the ratio m_t^4/m_W^4 and the terms $g^6\frac{m_t^6}{m_W^6}$ are also computed.

In the SM, the quantities Δr_W, $\Delta\rho$, Δk, for sufficiently large m_t, are all dominated by quadratic terms in m_t of order $G_F m_t^2$. The quantity $\Delta\rho_m$ is not independent and can be expressed in terms of them. As new physics can more easily be disentangled if not masked by large conventional m_t effects, it is convenient to keep $\Delta\rho$, while trading Δr_W and Δk for two quantities with no contributions of order $G_F m_t^2$. One thus introduces the following linear combinations (epsilon parameters) [48]:

$$\begin{aligned}
\epsilon_1 &= \Delta\rho \,, \\
\epsilon_2 &= c_0^2\Delta\rho + \frac{s_0^2}{c_0^2 - s_0^2}\Delta r_W - 2s_0^2\Delta k \,, \\
\epsilon_3 &= c_0^2\Delta\rho + (c_0^2 - s_0^2)\Delta k \,.
\end{aligned} \tag{3.106}$$

The quantities ϵ_2 and ϵ_3 no longer contain terms of order $G_F m_t^2$, but only logarithmic terms in m_t. The leading terms for large Higgs mass, which are logarithmic, are contained in ϵ_1 and ϵ_3. To complete the set of top-enhanced radiative corrections one adds ϵ_b, defined from the loop corrections to the $Zb\bar{b}$ vertex. One modifies g_V^b and g_A^b as follows:

$$g_A^b = -\frac{1}{2}\left(1 + \frac{\Delta\rho}{2}\right)(1 + \epsilon_b) \,, \qquad \frac{g_V^b}{g_A^b} = \frac{1 - \frac{4}{3}\sin^2\theta_{\rm eff} + \epsilon_b}{1 + \epsilon_b} \,. \tag{3.107}$$

ϵ_b can be measured from $R_b = \Gamma(Z \to b\bar{b})/\Gamma(Z \to \text{hadrons})$ (see Fig. 3.15). This is clearly not the most general deviation from the SM in the $Z \to b\bar{b}$ vertex, but ϵ_b is the quantity where the large m_t corrections are located in the SM. Thus, summarizing, in the SM one has the following "large" asymptotic contributions:

$$\begin{aligned}
\epsilon_1 &= \frac{3G_F m_t^2}{8\pi^2\sqrt{2}} - \frac{3G_F m_W^2}{4\pi^2\sqrt{2}}\tan^2\theta_W \ln\frac{m_H}{m_Z} + \cdots \,, \\
\epsilon_2 &= -\frac{G_F m_W^2}{2\pi^2\sqrt{2}}\ln\frac{m_t}{m_Z} + \cdots \,, \\
\epsilon_3 &= \frac{G_F m_W^2}{12\pi^2\sqrt{2}}\ln\frac{m_H}{m_Z} - \frac{G_F m_W^2}{6\pi^2\sqrt{2}}\ln\frac{m_t}{m_Z} + \cdots \,, \\
\epsilon_b &= -\frac{G_F m_t^2}{4\pi^2\sqrt{2}} + \cdots \,,
\end{aligned} \tag{3.108}$$

The ϵ_i parameters vanish in the limit where only tree level SM effects are kept plus pure QED and/or QCD corrections. So they describe the effects of quantum corrections (i.e., loops) from weak interactions. A similar set of parameters are the S, T, U parameters [310]: the shifts induced by new physics on S, T, and U are proportional to those induced on ϵ_3, ϵ_1, and ϵ_2, respectively. In principle, with no

model dependence, one can measure the four ϵ_i from the basic observables of LEP physics $\Gamma(Z \to \mu^+\mu^-)$, $A_{\rm FB}^{\mu}$, and R_b on the Z peak plus m_W. With increasing model dependence, one can include other measurements in the fit for the ϵ_i. For example, one can use lepton universality to average the μ with the e and τ final states, or include all lepton asymmetries and so on. The present experimental values of the ϵ_i, obtained from a fit of all LEP1-SLD measurements plus m_W, are [142]

$$\begin{aligned} \epsilon_1 \times 10^3 &= 5.6 \pm 1.0\,, \qquad \epsilon_2 \times 10^3 = -7.8 \pm 0.9\,, \\ \epsilon_3 \times 10^3 &= 5.6 \pm 0.9\,, \qquad \epsilon_b \times 10^3 = -5.8 \pm 1.3\,. \end{aligned} \tag{3.109}$$

Note that the ϵ parameters are of order a few 10^{-3} and are known with an accuracy in the range 15–30%. These values are in agreement with the predictions of the SM with a 126 GeV Higgs [142]:

$$\begin{aligned} \epsilon_1^{\rm SM} \times 10^3 &= 5.21 \pm 0.08\,, \qquad \epsilon_2^{\rm SM} \times 10^3 = -7.37 \pm 0.03\,, \\ \epsilon_3^{\rm SM} \times 10^3 &= 5.279 \pm 0.004\,, \qquad \epsilon_b^{\rm SM} \times 10^3 = -6.94 \pm 0.15\,. \end{aligned} \tag{3.110}$$

All models of new physics must be compared with these findings and pass this difficult test.

3.12 Results of the SM Analysis of Precision Tests

The electroweak Z pole measurements, combining the results of all the experiments, plus the W mass and width and the top mass m_t, are summarised in Fig 3.15, as of March 2012 [350]. The primary rates are given by the pole cross-sections for the various final states σ^0, and ratios thereof correspond to ratios of partial decay widths:

$$\sigma_{\rm h}^0 = \frac{12\pi}{m_Z^2}\,\frac{\Gamma_{ee}\Gamma_{\rm h}}{\Gamma_Z^2}\,, \qquad R_{\rm l}^0 = \frac{\sigma_{\rm h}^0}{\sigma_{\rm l}^0} = \frac{\Gamma_{\rm h}}{\Gamma_{\rm ll}}\,, \qquad R_q^0 = \frac{\Gamma_{q\bar{q}}}{\Gamma_{\rm h}}\,. \tag{3.111}$$

Here $\Gamma_{\rm ll}$ is the partial decay width for a pair of massless charged leptons. The partial decay width for a given fermion species contains information about the effective vector and axial-vector coupling constants of the neutral weak current:

$$\Gamma_{ff} = N_{\rm C}^f \frac{G_{\rm F} m_Z^3}{6\sqrt{2}\pi}\left(g_{{\rm a}f}^2 C_{{\rm A}f} + g_{{\rm v}f}^2 C_{{\rm V}f}\right) + \Delta_{\rm ew/QCD}\,, \tag{3.112}$$

where $N_{\rm C}^f$ is the QCD colour factor, $C_{\{{\rm A,V}\}f}$ are final-state QCD/QED correction factors, also absorbing imaginary contributions to the effective coupling constants,

g_{af} and g_{vf} are the real parts of the effective couplings, and Δ contains non-factorisable mixed corrections.

Besides total cross-sections, various types of asymmetries have been measured. The results of all asymmetry measurements are quoted in terms of the asymmetry parameter A_f, defined in terms of the real parts of the effective coupling constants g_{af} and g_{vf} by

$$A_f = 2\frac{g_{vf}g_{af}}{g_{vf}^2 + g_{af}^2} = 2\frac{g_{vf}/g_{af}}{1 + (g_{vf}/g_{af})^2} , \qquad A_{FB}^{0,f} = \frac{3}{4}A_e A_f . \tag{3.113}$$

The measurements are the forward–backward asymmetry ($A_{FB}^{0,f}$), the tau polarization (A_τ) and its forward–backward asymmetry (A_e) measured at LEP, as well as the left–right and left–right forward–backward asymmetry measured at SLC (A_e and A_f, respectively). Hence the set of partial width and asymmetry results allows the extraction of the effective coupling constants.

The various asymmetries determine the effective electroweak mixing angle for leptons with highest sensitivity (see Fig. 3.16). The weighted average of these results, including small correlations, is

$$\sin^2\theta_{\text{eff}} = 0.23153 \pm 0.00016 , \tag{3.114}$$

Note, however, that this average has a χ^2 of 11.8 for 5 degrees of freedom, corresponding to a probability of a few %. The χ^2 is pushed up by the two most precise measurements of $\sin^2\theta_{\text{eff}}$, namely those derived from the measurements of A_l by SLD, dominated by the left–right asymmetry A_{LR}^0, and measurements of the forward–backward asymmetry $A_{FB}^{0,b}$ measured in $b\bar{b}$ production at LEP, which differ by about 3σ.

We now extend the discussion of the SM fit of the data. One can think of different types of fit, depending on which experimental results are included or which answers one wants to obtain. For example, in Table 3.2 we present in column 1 a fit of all Z pole data plus m_W and Γ_W (this is interesting as it shows the value of m_t obtained

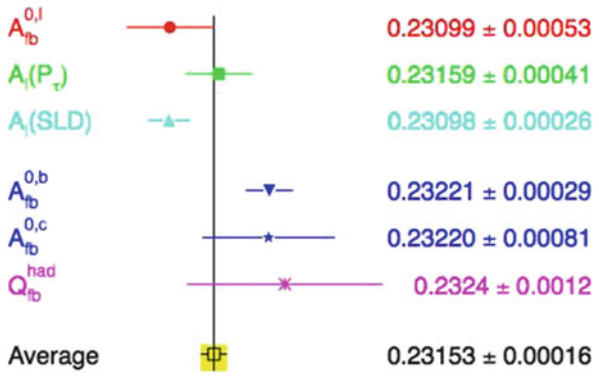

Fig. 3.16 Summary of $\sin^2\theta_{\text{eff}}$ precision measurements at high Q^2 [350]

Table 3.2 Standard Model fits of electroweak data [350]

Fit	1	2	3
Measurements	m_W, Γ_W	m_t	m_t, m_W, Γ_W
m_t (GeV)	$178.1^{+10.9}_{-7.8}$	173.2 ± 0.9	173.26 ± 0.89
$m_{\rm H}$ (GeV)	148^{+237}_{-81}	122^{+59}_{-41}	94^{+29}_{-24}
log $[m_{\rm H}({\rm GeV})]$	$2.17 \pm +0.38$	2.09 ± 0.17	1.97 ± 0.12
$\alpha_{\rm s}(m_Z)$	0.1190 ± 0.0028	0.1191 ± 0.0027	0.1185 ± 0.0026
m_W (MeV)	80381 ± 13	80363 ± 20	80377 ± 12

All fits use the Z pole results and $\Delta\alpha^{(5)}_{\rm had}(m_Z^2)$, as listed in Fig. 3.15. In addition, the measurements listed at the top of each column are included in that case. The fitted W mass is also shown [350] (the directly measured value is $m_W = 80\,385 \pm 15\,{\rm MeV}$)

indirectly from radiative corrections, to be compared with the value of m_t measured in production experiments), in column 2, a fit of all Z pole data plus m_t (here it is m_W which is indirectly determined), and finally, in column 3, a fit of all the data listed in Fig. 3.15 (which is the most relevant fit for constraining $m_{\rm H}$).

From the fit in column 1 we see that the extracted value of m_t is in good agreement with the direct measurement (see Fig 3.15). Similarly, we see that the experimental measurement of m_W is larger by about one standard deviation with respect to the value from the fit in column 2. We have seen that quantum corrections depend only logarithmically on $m_{\rm H}$. In spite of this small sensitivity, the measurements are still precise enough to obtain a quantitative indication of the mass range. From the fit in column 3 we obtain

$$\log_{10} m_{\rm H}\,({\rm GeV}) = 1.97 \pm 0.12\,, \quad \text{or } m_{\rm H} = 94^{+29}_{-24}\,{\rm GeV}\,.$$

This result on the Higgs mass is truly remarkable. The value of $\log_{10} m_{\rm H}$ (GeV) is compatible with the small window between ~ 2 and ~ 3 which is allowed, on the one side, by the direct search limit $m_{\rm H} > 114\,{\rm GeV}$ from LEP2 [350], and on the other side by the theoretical upper limit on the Higgs mass in the minimal SM, $m_{\rm H} \lesssim 600$–$800\,{\rm GeV}$ [320], to be discussed in Sect. 3.13.

Thus the whole picture of a perturbative theory with a fundamental Higgs is well supported by the data on radiative corrections. It is important that there is a clear indication for a particularly light Higgs: at 95% confidence level $m_{\rm H} \lesssim 152\,{\rm GeV}$ (which becomes $m_{\rm H} \lesssim 171\,{\rm GeV}$, including the input from the LEP2 direct search result). This was quite encouraging for the LHC search for the Higgs particle. More generally, if the Higgs couplings are removed from the Lagrangian, the resulting theory is non-renormalizable. A cutoff Λ must be introduced. In the quantum corrections, $\log m_{\rm H}$ is then replaced by $\log \Lambda$ plus a constant. The precise determination of the associated finite terms would be lost (that is, the value of the mass in the denominator in the argument of the logarithm). A heavy Higgs would need some unfortunate accident: the finite terms, different in the new theory from those of the SM, should by chance compensate for the heavy Higgs in a few

key parameters of the radiative corrections (mainly ϵ_1 and ϵ_3, see, for example, [48]). Alternatively, additional new physics, for example in the form of effective contact terms added to the minimal SM Lagrangian, should accidentally do the compensation, which again needs some sort of conspiracy.

To the list of precision tests of the SM, one should add the results on low energy tests obtained from neutrino and antineutrino deep inelastic scattering (NuTeV [353]), parity violation in Cs atoms (APV [274]), and the recent measurement of the parity-violating asymmetry in Moller scattering [354]. When these experimental results are compared with the SM predictions, the agreement is good except for the NuTeV result, which differs by three standard deviations. The NuTeV measurement is quoted as a measurement of $\sin^2\theta_{\rm W} = 1 - m_W^2/m_Z^2$ from the ratio of neutral to charged current deep inelastic cross-sections from ν_μ and $\bar{\nu}_\mu$ using the Fermilab beams. But it has been argued, and it is now generally accepted, that the NuTeV anomaly probably simply arises from an underestimation of the theoretical uncertainty in the QCD analysis needed to extract $\sin^2\theta_{\rm W}$. In fact, the lowest order QCD parton formalism upon which the analysis has been based is too crude to match the experimental accuracy.

When confronted with these results, the SM performs rather well on the whole, so that it is fair to say that no clear indication for new physics emerges from the data. However, as already mentioned, one problem is that the two most precise measurements of $\sin^2\theta_{\rm eff}$ from $A_{\rm LR}$ and $A_{\rm FB}^b$ differ by about 3σ. In general, there appears to be a discrepancy between $\sin^2\theta_{\rm eff}$ measured from leptonic asymmetries, denoted $(\sin^2\theta_{\rm eff})_{\rm l}$, and from hadronic asymmetries, denoted $(\sin^2\theta_{\rm eff})_{\rm h}$. In fact, the result from $A_{\rm LR}$ is in good agreement with the leptonic asymmetries measured at LEP, while all hadronic asymmetries, though their errors are large, are better compatible with the result of $A_{\rm FB}^b$. These two results for $\sin^2\theta_{\rm eff}$ are shown in Fig. 3.17 [210]. Each of them is plotted at the $m_{\rm H}$ value that would correspond to it given the central value of m_t. Of course, the value for $m_{\rm H}$ indicated by each $\sin^2\theta_{\rm eff}$ has a horizontal ambiguity determined by the measurement error and the width of the $\pm 1\sigma$ band for m_t.

Even taking this spread into account, it is clear that the implications for $m_{\rm H}$ are significantly different. One might imagine that some new physics effect could be hidden in the $Zb\bar{b}$ vertex. For instance, for the top quark mass there could be other non-decoupling effects from new heavy states or a mixing of the b quark with some other heavy quark. However, it is well known that this discrepancy is not easily explained in terms of any new physics effect in the $Zb\bar{b}$ vertex. A rather large change with respect to the SM of the b quark right-handed coupling to the Z is needed in order to reproduce the measured discrepancy (in fact, a $\sim 30\%$ change in the right-handed coupling), an effect too large to be a loop effect, but which could be produced at the tree level, e.g., by mixing of the b quark with a new heavy vector-like quark [140], or some mixing of the Z with ad hoc heavy states [170]. But then this effect should normally also appear in the direct measurement of A_b performed at SLD using the left–right polarized b asymmetry, even within the moderate accuracy of this result. The measurements of neither A_b at SLD nor R_b confirm the need for

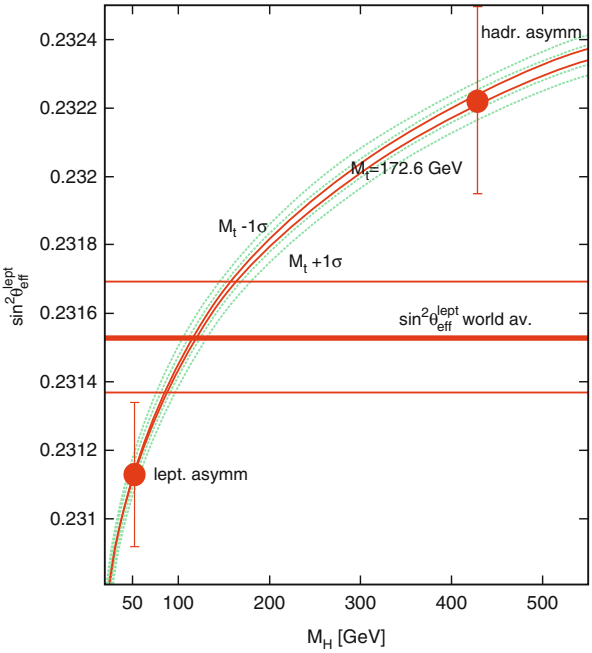

Fig. 3.17 The data for $\sin^2\theta_{\rm eff}^{\rm lept}$ are plotted vs $m_{\rm H}$. The theoretical prediction for the measured value of m_t is also shown. For presentation purposes the measured points are each shown at the $m_{\rm H}$ value that would ideally correspond to it, given the central value of m_t. Adapted from [210]. New version courtesy of P. Gambino

such a large effect (recently a numerical calculation of NLO corrections to R_b [204] appeared at first to indicate a rather large result, but in the end the full correction turned out to be rather small). Alternatively, the observed discrepancy could simply be due to a large statistical fluctuation or an unknown experimental problem. As a consequence of this problem, the ambiguity in the measured value of $\sin^2\theta_{\rm eff}$ is in practice greater than the nominal error, reported in (3.114), obtained from averaging all the existing determinations, and the interpretation of precision tests is less sharp than it would otherwise be.

We have already observed that the experimental value of m_W (with good agreement between LEP and the Tevatron) is a bit high compared to the SM prediction (see Fig. 3.18). The value of $m_{\rm H}$ indicated by m_W is on the low side, just in the same interval as for $\sin^2\theta_{\rm eff}^{\rm lept}$ measured from leptonic asymmetries.

In conclusion, the experimental information on the Higgs sector, obtained from EW precision tests at LEP1 and 2 and the Tevatron can be summarized as follows. First, the relation $M_W^2 = M_Z^2\cos^2\theta_{\rm W}$ in (3.52), modified by small, computable radiative corrections, has been demonstrated experimentally. This relation means that the effective Higgs (be it fundamental or composite) is indeed a weak isospin doublet. The direct lower limit $m_{\rm H} \gtrsim 114.5\,\text{GeV}$ (at 95% confidence level) was

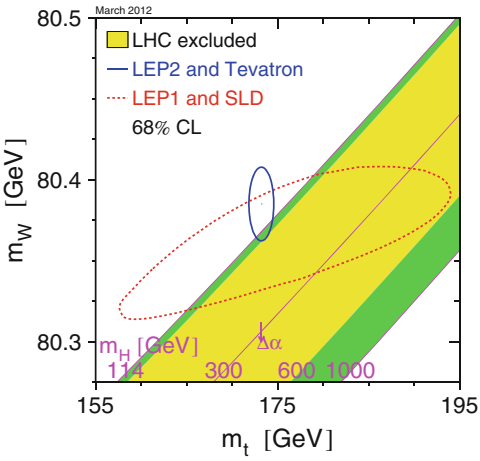

Fig. 3.18 The data for m_W are plotted vs m_t [350]

obtained from searches at LEP2. When compared to the data on precision EW tests, the radiative corrections computed in the SM lead to a clear indication of a light Higgs, not too far from the direct LEP2 lower bound. The upper limit for m_{H} in the SM from the EW tests depends on the value of the top quark mass m_t. The CDF and D0 combined value after Run II is at present $m_t = 173.2 \pm 0.9\,\mathrm{GeV}$ [350]. As a consequence, the limit on m_{H} from the LEP and Tevatron measurements is rather stringent [350]: $m_{\mathrm{H}} < 171\,\mathrm{GeV}$ (at 95% confidence level, after including the information from the 114.5 GeV direct bound).

3.13 The Search for the SM Higgs

The Higgs problem is really central in particle physics today. On the one hand, the experimental verification of the Standard Model (SM) cannot be considered complete until the structure of the Higgs sector has been established by experiment. On the other hand, the Higgs is also related to most of the major problems of particle physics, like the flavour problem and the hierarchy problem, the latter strongly suggesting the need for new physics near the weak scale (something that so far has not been found). In its turn, the discovery of new physics could throw light on the nature of dark matter. It was already clear before the LHC that some sort of Higgs mechanism is at work. The W or the Z with longitudinal polarization that we observe are not present in an unbroken gauge theory (massless spin-1 particles, like the photon, are transversely polarized): the longitudinal degrees of freedom for the W or the Z are borrowed from the Higgs sector and hence provide evidence for it.

Furthermore, it has been precisely established at LEP that the gauge symmetry is unbroken in the vertices of the theory: all currents and charges are indeed symmetric. Yet there is obvious evidence that the symmetry is instead badly broken in the

masses. Not only do the W and the Z have large masses, but the large splitting of, for example, the t–b doublet shows that even a global weak $SU(2)$ is not at all respected by the fermion spectrum. This is a clear signal of spontaneous symmetry breaking and the implementation of spontaneous symmetry breaking in a gauge theory is via the Higgs mechanism.

The big questions are about the nature and the properties of the Higgs particle(s). The search for the Higgs boson and for possible new physics that could accompany it was the main goal of the LHC from the start. On the Higgs the LHC should answer the following questions: do some Higgs particles exist? And if so, which ones: a single doublet, more doublets, additional singlets? SM Higgs or SUSY Higgses? Fundamental or composite (of fermions, of WW, or other)? Pseudo-Goldstone bosons of an enlarged symmetry? A manifestation of large extra dimensions (fifth component of a gauge boson, an effect of orbifolding or of boundary conditions, or other)? Or some combination of the above, or something so far unthought of? By now we have a candidate Higgs boson that really looks like the simplest realization of the Higgs mechanism, as described by the minimal SM Higgs. In the following we first consider the a priori expectations for the Higgs sector and then the profile of the Higgs candidate discovered at the LHC.

3.14 Theoretical Bounds on the SM Higgs Mass

A strong argument indicating that the solution of the Higgs problem may not be too far away (that is, either discovering the Higgs or finding the new physics that complicates the picture) is the fact that, in the absence of a Higgs particle or any alternative mechanism, violations of unitarity appear in some scattering amplitudes at energies in the few TeV range [279]. In particular, amplitudes involving longitudinal gauge bosons (those most directly related to the Higgs sector) are affected. For example, at tree level, in the absence of Higgs exchange and for $s \gg m_Z^2$, one obtains

$$A(W_L^+ W_L^- \to Z_L Z_L)_{\text{no Higgs}} \sim \mathrm{i}\frac{s}{v^2} \,. \tag{3.115}$$

In the SM this unacceptable large energy behaviour is quenched by the Higgs exchange diagram contribution

$$A(W_L^+ W_L^- \to Z_L Z_L)_{\text{Higgs}} \sim -\mathrm{i}\frac{s^2}{v^2(s - m_H^2)} \,. \tag{3.116}$$

Thus the total result in the SM is

$$A(W_L^+ W_L^- \to Z_L Z_L)_{SM} \sim -i\frac{s m_H^2}{v^2(s - m_H^2)} \,, \tag{3.117}$$

which at high energies saturates at a constant value. To be compatible with unitarity bounds, one needs $m_{\rm H}^2 < 4\pi\sqrt{2}/G_{\rm F}$ or $m_{\rm H} < 1.5\,{\rm TeV}$. This is an important theorem that guarantees that either the Higgs boson(s) or new physics or both must be present in the few TeV energy range.

It is well known that, as described in [241] and references therein, in the SM with only one Higgs doublet an upper bound on $m_{\rm H}$ (with mild dependence on m_t and the QCD coupling $\alpha_{\rm s}$) is obtained from the requirement that the perturbative description of the theory remains valid up to a large energy scale Λ where the SM model breaks down and new physics appears. Similarly, a lower bound on $m_{\rm H}$ can be derived from the requirement of vacuum stability [38, 123, 323] (or, in milder form, a requirement of moderate instability, compatible with the lifetime of the Universe [160, 249]). The Higgs mass enters because it fixes the initial value of the quartic Higgs coupling λ in its running up to the large scale Λ. We now briefly recall the derivation of these limits.

The upper limit on the Higgs mass in the SM is clearly important for an a priori assessment of the chances of success for the LHC as an accelerator designed to solve the Higgs problem. One way to estimate the upper limit [241] is to require that the Landau pole associated with the non-asymptotically free behaviour of the $\lambda\phi^4$ theory does not occur below the scale Λ. The running of $\lambda(\Lambda)$ at one loop is given by

$$\frac{{\rm d}\lambda}{{\rm d}t} = \frac{3}{4\pi^2}\left[\lambda^2 + 3\lambda h_t^2 - 9h_t^4 + \text{small gauge and Yukawa terms}\right], \tag{3.118}$$

with the normalization such that at $t = 0$, $\lambda = \lambda_0 = m_H^2/2v^2$, from the minimum condition in (3.60), and the top Yukawa coupling is given by $h_t^0 = m_t/v$. The initial value of λ at the weak scale increases with $m_{\rm H}$ and the derivative is positive at large λ because of the positive λ^2 term (the $\lambda\varphi^4$ theory is not asymptotically free), which overwhelms the negative top Yukawa term. Thus, if $m_{\rm H}$ is too large, the point where λ computed from the perturbative beta function becomes infinite (the Landau pole) occurs at too low an energy. Of course, in the vicinity of the Landau pole the 2-loop evaluation of the beta function is not reliable. Indeed, the limit indicates the frontier of the domain where the theory is well described by the perturbative expansion. Thus the quantitative evaluation of the limit is only indicative, although it has been to some extent supported by simulations of the Higgs sector of the EW theory on the lattice. For the upper limit on $m_{\rm H}$, one finds [241]

$$m_{\rm H} \lesssim 180\,{\rm GeV} \ \text{ for } \Lambda \sim M_{\rm GUT}\text{–}M_{\rm Planck}\,, \quad m_{\rm H} \lesssim 0.5\text{–}0.8\,{\rm TeV} \ \text{ for } \Lambda \sim 1\,{\rm TeV}\,. \tag{3.119}$$

As for a lower limit on the SM Higgs mass, a possible instability of the Higgs potential $V[\phi]$ is generated by the quantum loop corrections to the classical expression for $V[\phi]$. At large ϕ the derivative $V'[\phi]$ could become negative and the potential would become unbound from below. The one-loop corrections to $V[\phi]$ in the SM are well known and change the dominant term at large ϕ according to

$\lambda\phi^4 \to (\lambda + \gamma \log \phi^2/\Lambda^2)\phi^4$. This one-loop approximation is not enough in this case, because it fails at large enough ϕ, when $\gamma \log \phi^2/\Lambda^2$ becomes of order 1. The renormalization group improved version of the corrected potential leads to the replacement $\lambda\phi^4 \to \lambda(\Lambda)\phi'^4(\Lambda)$, where $\lambda(\Lambda)$ is the running coupling and $\phi'(\mu) = \phi \exp \int^t \gamma(t')\mathrm{d}t'$, with $\gamma(t)$ an anomalous dimension function, $t = \log \Lambda/v$, and v the vacuum expectation value $v = (2\sqrt{2}G_\mathrm{F})^{-1/2}$. As a result, the positivity condition for the potential amounts to the requirement that the running coupling $\lambda(\Lambda)$ should never become negative.

A more precise calculation, which also takes into account the quadratic term in the potential, confirms that the requirement of positive $\lambda(\Lambda)$ leads to the correct bound down to scales Λ as low as ~ 1 TeV. We see that, for m_H small and m_t fixed at its measured value, λ decreases with t and can become negative. If one requires λ to remain positive up to $\Lambda = 10^{16}$–10^{19} GeV, then the resulting bound on m_H in the SM with only one Higgs doublet, obtained from a recent state-of-the-art calculation [118, 160] is given by

$$m_\mathrm{H}\,(\mathrm{GeV}) > 129.6 + 2.0\left[\frac{m_t\,(\mathrm{GeV}) - 173.35}{0.7}\right] - 0.5\frac{\alpha_\mathrm{s}(m_Z) - 0.1184}{0.0007} \pm 0.3\ . \tag{3.120}$$

The estimate of the ambiguity associated with m_t can be questioned: is the definition of mass as measured at the Tevatron relevant for this calculation [25]? Note that this limit is avoided in models with more Higgs doublets. In that case the limit, applies to some average mass, but the lightest Higgs particle can be well below, as is the case in the minimal SUSY extension of the SM (MSSM).

In conclusion, for $m_t \sim 173$ GeV, only a small range of values for m_H is allowed, viz., $130 < m_\mathrm{H} <\sim 180$ GeV, if the SM holds and the vacuum is absolutely stable up to an energy scale $\Lambda \sim M_\mathrm{GUT}$ or M_Planck. For Higgs masses below this range, one can still have a domain where the SM is viable because the vacuum can be unstable, but with a lifetime longer than the age of the Universe [111, 118, 160]. We shall come back to this later (see Fig. 3.21).

3.15 SM Higgs Decays

The total width and the branching ratios for the SM Higgs as a function of m_H are given in Fig. 3.19 [169]. Since the couplings of the Higgs particle are proportional to masses, when m_H increases, the Higgs particle becomes strongly coupled. This is reflected in the sharp rise of the total width with m_H. For m_H in the range 114–130 GeV, the width is below 5 MeV, much less than the widths of the W or the Z, which have a comparable mass. The dominant channel for such a Higgs is $H \to b\bar{b}$. In the Born approximation, the partial width into a fermion pair is given

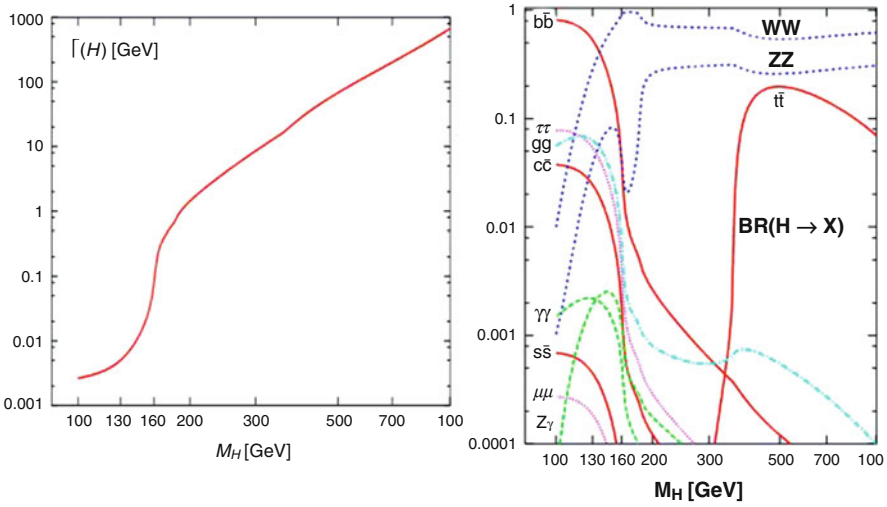

Fig. 3.19 *Left*: The total width of the SM Higgs boson as a function of the mass. *Right*: The branching ratios of the SM Higgs boson as a function of the mass (*solid line* fermions, *dashed line* bosons) [169]

by [169, 238]

$$\Gamma(H \to f\bar{f}) = N_{\mathrm{C}} \frac{G_{\mathrm{F}}}{4\pi\sqrt{2}} m_{\mathrm{H}} m_f^2 \beta_f^3 \,, \tag{3.121}$$

where $\beta_f = (1 - 4m_f^2/m_{\mathrm{H}}^2)^{1/2}$. The factor of β^3 appears because parity requires the fermion pair to be in a p-state of orbital angular momentum for a scalar Higgs (with parity $P = +1$). This factor would be β for a pseudoscalar Higgs boson. We see that the width is suppressed by a factor m_f^2/m_{H}^2 (the Higgs coupling is proportional to the fermion mass) with respect to the natural size $G_{\mathrm{F}} m_{\mathrm{H}}^3$ for the width of a particle of mass m_{H} decaying through a diagram with only one weak vertex.

A glance at the branching ratios shows that the branching ratio into τ pairs is larger by more than a factor of 2 with respect to the $c\bar{c}$ channel. This is at first sight surprising because the colour factor N_{C} favours the quark channels and the masses of τ leptons and D mesons are quite similar. This is due to the fact that the QCD corrections replace the charm mass at the scale of charm with the charm mass at the scale m_{H}, which is lower by about a factor of 2.5. The masses run logarithmically in QCD, similarly to the coupling constant. The corresponding logs are already present in the 1-loop QCD correction, which amounts to the replacement

$$m_q^2 \longrightarrow m_q^2 \left[1 + \frac{2\alpha_{\mathrm{s}}}{\pi} \left(\log \frac{m_q^2}{m_{\mathrm{H}}^2} + \frac{3}{2} \right) \right] \sim m_q^2(m_{\mathrm{H}}^2) \,.$$

The Higgs width increases sharply as the WW threshold is approached. For decay into a real pair of V bosons, with $V = W, Z$, one obtains in the Born approximation [169, 238]

$$\Gamma(H \to VV) = \frac{G_F m_H^3}{16\pi\sqrt{2}} \delta_V \beta_V (1 - 4x + 12x^2) \,, \tag{3.122}$$

where $\beta_V = \sqrt{1-4x}$ with $x = m_V^2/m_H^2$ and $\delta_W = 2$, $\delta_Z = 1$. Well above threshold, the VV channels are dominant and the total width, given approximately by

$$\Gamma_H \sim 0.5 \text{ TeV} \left(\frac{m_H}{1 \text{ TeV}}\right)^3 \,, \tag{3.123}$$

becomes very large, signalling that the Higgs sector is becoming strongly interacting, if we recall the upper limit on the SM Higgs mass in (3.119). The VV dominates over the $t\bar{t}$ because of the β threshold factors, which disfavour the fermion channel, and at large m_H, by the cubic versus linear behaviour with m_H of the partial widths for VV versus $t\bar{t}$. Below the VV threshold, the decays into virtual V particles is important: VV^* and V^*V^*. Note in particular the dip in the ZZ branching ratio just below the ZZ threshold. This is due to the fact that the W is lighter than the Z and the opening of its threshold depletes all other branching ratios. When the ZZ threshold is also passed, the ZZ branching fraction then comes back to the ratio of approximately 1:2 with the WW channel (just the number of degrees of freedom, i.e., two Hermitian fields for the W, one for the Z). The decay channels into $\gamma\gamma$, $Z\gamma$, and gg proceed through loop diagrams, with the contributions from W (only for $\gamma\gamma$ and $Z\gamma$) and from fermion loops (for all) (Fig. 3.20).

We reproduce here the results for $\Gamma(H \to \gamma\gamma)$ and $\Gamma(H \to gg)$ [169, 238]:

$$\Gamma(H \to \gamma\gamma) = \frac{G_F \alpha^2 m_H^3}{128\pi^3\sqrt{2}} \left| A_W(\tau_W) + \sum_f N_C Q_f^2 A_f(\tau_f) \right|^2 \,, \tag{3.124}$$

$$\Gamma(H \to gg) = \frac{G_F \alpha_s^2 m_H^3}{64\pi^3\sqrt{2}} \left| \sum_{f=Q} A_f(\tau_f) \right|^2 \,, \tag{3.125}$$

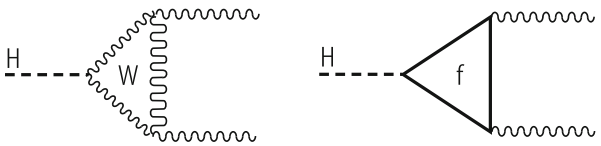

Fig. 3.20 Typical one-loop diagrams for Higgs decay into $\gamma\gamma$, $Z\gamma$, and for only the quark loop, gg

where $\tau_i = m_{\rm H}^2/4m_i^2$ and

$$A_f(\tau) = \frac{2}{\tau^2}\big[\tau + (\tau-1)f(\tau)\big]\,, \quad A_W(\tau) = -\frac{1}{\tau^2}\big[2\tau^2 + 3\tau + 3(2\tau-1)f(\tau)\big]\,, \tag{3.126}$$

with

$$f(\tau) = \begin{cases} \arcsin^2\sqrt{\tau} & \text{for } \tau \le 1\,, \\ -\dfrac{1}{4}\left(\log\dfrac{1+\sqrt{1-\tau^{-1}}}{1-\sqrt{1-\tau^{-1}}} - {\rm i}\pi\right)^2 & \text{for } \tau > 1\,. \end{cases} \tag{3.127}$$

For $H \to \gamma\gamma$ (as well as for $H \to Z\gamma$), the W loop is the dominant contribution at small and moderate $m_{\rm H}$. We recall that the $\gamma\gamma$ mode is a possible channel for Higgs discovery only for $m_{\rm H}$ near its lower bound (i.e., for $114 < m_{\rm H} < 150\,{\rm GeV}$). In this domain of $m_{\rm H}$, we have $\Gamma(H \to \gamma\gamma) \sim 6$–$23\,{\rm KeV}$. For example, in the limit $m_{\rm H} \ll 2m_i$, or $\tau \to 0$, we have $A_W(0) = -7$ and $A_f(0) = 4/3$. The two contributions become comparable only for $m_{\rm H} \sim 650\,{\rm GeV}$, where the two amplitudes, still of opposite sign, nearly cancel. The top loop is dominant among fermions (lighter fermions are suppressed by $m_f^2/m_{\rm H}^2$ modulo logs), and as we have seen, it approaches a constant for large m_t. Thus the fermion loop amplitude for the Higgs would be sensitive to effects from very heavy fermions. In particular, the $H \to gg$ effective vertex would be sensitive to all possible very heavy coloured quarks (of course, there is no W loop in this case, and the top quark gives the dominant contribution in the loop). As discussed in Chap. 2, the $gg \to H$ vertex provides one of the main production channels for the Higgs boson at hadron colliders, while another important channel at present is WH associate production.

3.16 The Higgs Discovery at the LHC

On 4 July 2012 at CERN, the ATLAS and CMS Collaborations [341, 345] announced the observation of a particle with mass around 126 GeV that, within the present accuracy, does indeed look like the SM Higgs boson. This is a great breakthrough which, by itself, already makes an adequate return for the LHC investment. With the Higgs discovery, the main building block for the experimental validation of the SM is now in place. The Higgs discovery is the last milestone in the long history (some 130 years) of the development of a field theory of fundamental interactions (apart from quantum gravity), starting with the Maxwell equations of classical electrodynamics, going through the great revolutions of relativity and quantum mechanics, then the formulation of quantum electrodynamics (QED) and the gradual buildup of the gauge part of the Standard Model, and finally completed with the tentative description of the electroweak (EW) symmetry breaking sector of

the SM in terms of a simple formulation of the Englert–Brout–Higgs mechanism [189].

The other extremely important result from the LHC at 7 and 8 TeV center-of-mass energy is that no new physics signals have been seen so far. This negative result is certainly less exciting than a positive discovery, but it is a crucial new input which, if confirmed in the future LHC runs at 13 and 14 TeV, will be instrumental in redirecting our perspective of the field. In this section we summarize the relevant data on the Higgs signal as they are known at present, while the analysis of the data from the 2012 LHC run is still in progress.

The Higgs particle has been observed by ATLAS and CMS in five channels $\gamma\gamma$, ZZ^*, WW^*, $b\bar{b}$, and $\tau^+\tau^-$. If we also include the Tevatron experiments, especially important for the $b\bar{b}$ channel, the combined evidence is by now totally convincing. The ATLAS (CMS) combined values for the mass, in GeV$/c^2$, are $m_{\rm H} = 125.5\pm0.6$ ($m_{\rm H} = 125.7\pm0.4$). This light Higgs is what one expects from a direct interpretation of EW precision tests [73, 142, 350]. The possibility of a "conspiracy" (the Higgs is heavy, but it falsely appears to be light because of confusing new physics effects) has been discarded: the EW precision tests of the SM tell the truth and in fact, consistently, no "conspirators", namely no new particles, have been seen around.

As shown in the previous section, the observed value of $m_{\rm H}$ is a bit too low for the SM to be valid up to the Planck mass with an absolutely stable vacuum [see (3.120)], but it corresponds to a metastable value with a lifetime longer than the age of the universe, so that the SM may well be valid up to the Planck mass (if one is ready to accept the immense fine-tuning that this option implies, as discussed in Sect. 3.17). This is shown in Fig. 3.21, where the stability domains are shown as functions of m_t and $m_{\rm H}$, as obtained from a recent state-of-the-art evaluation of the relevant boundaries [118, 160]. It is puzzling to find that, with the measured values of the top and Higgs masses and the strong coupling constant, the evolution of the Higgs quartic coupling ends up in a narrow metastability wedge at very high energies. This criticality looks intriguing, and is perhaps telling us something.

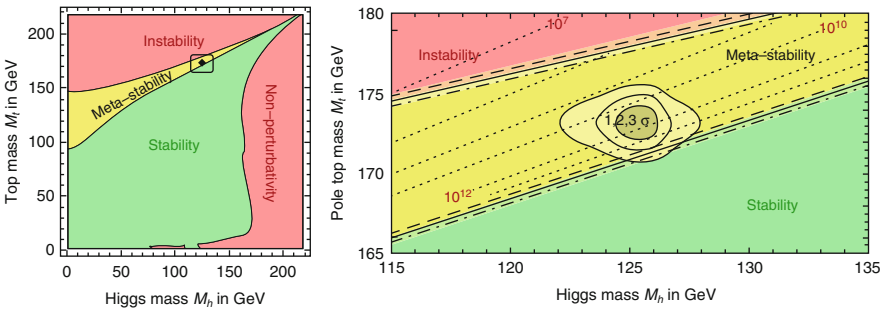

Fig. 3.21 Vacuum stability domains in the SM for the observed values of m_t and $m_{\rm H}$ [118, 160]. *Right*: Expanded view of the most relevant domain in the m_t–$m_{\rm H}$ plane. *Dotted contour lines* show the scale Λ in GeV where the instability sets in, for $\alpha_{\rm s}(m_Z) = 0.1184$

In order to be sure that this is the SM Higgs boson, one must confirm that the spin-parity is 0^+ and that the couplings are as predicted by the theory. It is also essential to search for possible additional Higgs states, such as those predicted in supersymmetric extensions of the SM. As for the spin (see, for example, [179]), the existence of the $H \to \gamma\gamma$ mode proves that the spin cannot be 1, and must be either 0 or 2, in the assumption of an s-wave decay. The $b\bar{b}$ and $\tau^+\tau^-$ modes are compatible with both possibilities. With large enough statistics the spin-parity can be determined from the distributions of $H \to ZZ^* \to 4$ leptons, or $WW^* \to 4$ leptons. Information can also be obtained from the HZ invariant mass distributions in the associated production [179]. The existing data already appear to strongly favour a $J^P = 0^+$ state against 0^-, $1^{+/-}$, or 2^+ [68]. We do not expect surprises on the spin-parity assignment because, if different, then all the Lagrangian vertices would be changed and the profile of the SM Higgs particle would be completely altered.

The tree level couplings of the Higgs are proportional to masses, and as a consequence are very hierarchical. The loop effective vertices to $\gamma\gamma$ and gg, g being the gluon, are also completely specified in the SM, where no states heavier than the top quark exist and contribute in the loop. This means that the SM Higgs couplings are predicted to exhibit a very special and very pronounced pattern (see Fig. 3.22) which would be extremely difficult to fake by a random particle. In fact, only a dilaton, a particle coupled to the energy–momentum tensor, could come close to simulating a Higgs particle, at least for the H tree level couplings, although in general there would be a common proportionality factor in the couplings. The hierarchy of couplings is reflected in the branching ratios and the rates of production channels, as can be seen in Fig. 3.23. The combined signal strengths (which, modulo acceptance and selection cut deformations, correspond to $\mu = \sigma Br/(\sigma Br)_{\rm SM}$) are obtained as $\mu = 0.8 \pm 0.14$ by CMS and $\mu = 1.30 \pm 0.20$ by ATLAS. Taken together these numbers constitute a triumph for the SM!

Within the somewhat limited present accuracy (October 2013), the measured Higgs couplings are in reasonable agreement (at about a 20% accuracy) with the

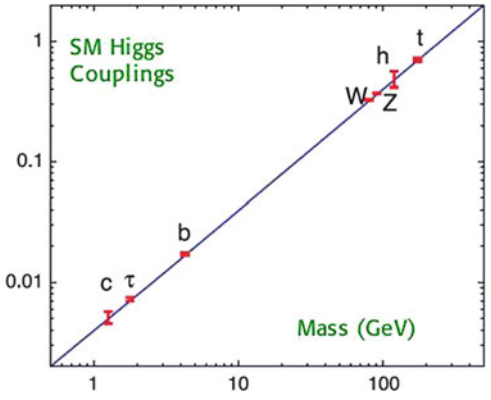

Fig. 3.22 Predicted couplings of the SM Higgs

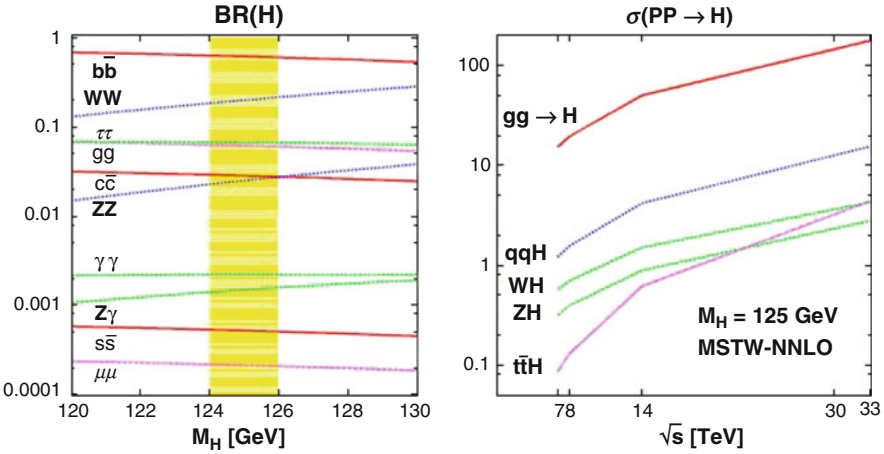

Fig. 3.23 Branching ratios of the SM Higgs boson in the mass range $m_{\mathrm{H}} = 120$–$130\,\mathrm{GeV}$ (*left*) and its production cross-sections at the LHC for various center-of-mass energies (*right*) [168]

sharp predictions of the SM. Great interest was excited by a hint of an enhanced Higgs signal in $\gamma\gamma$, but if we put the ATLAS and CMS data together, the evidence appears now to have evaporated. All included, if the CERN particle is not the SM Higgs, it must be a very close relative! Still it would be really astonishing if the H couplings were exactly those of the minimal SM, meaning that no new physics distortions reach an appreciable level of contribution.

Thus, it becomes a firm priority to establish a roadmap for measuring the H couplings as precisely as possible. The planning of new machines beyond the LHC has already started. Meanwhile strategies for analyzing the already available and the forthcoming data in terms of suitable effective Lagrangians have been formulated (see, for example, [222] and references therein). A very simple test is to introduce a universal factor multiplying all $H\bar{\psi}\psi$ couplings to fermions, denoted by c, and another factor a multiplying the HWW and HZZ vertices. Both a and c are 1 in the SM limit. All existing data on production times branching ratios are compared with the a- and c-distorted formulae to obtain the best fit values of these parameters (see [72, 194, 218] and references therein). At present this fit is performed routinely by the experimental collaborations [66, 260], each using its own data (see Fig. 3.24). But theorists have not refrained from abusively combining the data from both experiments and the result is well in agreement with the SM, as shown in Fig. 3.25 [194, 218].

Actually, a more ambitious fit in terms of seven parameters has also been performed [194] with a common factor like a for couplings to WW and ZZ, three separate c-factors c_t, c_b, and c_τ for u-type and d-type quarks and for charged leptons, and three parameters c_{gg}, $c_{\gamma\gamma}$, and $c_{Z\gamma}$ for additional gluon–gluon, γ–γ and Z–γ terms, respectively. In the SM $a = c_t = c_b = c_\tau = 1$ and $c_{gg} = c_{\gamma\gamma} = c_{Z\gamma} = 0$. The present data allow a meaningful determination of all seven parameters which

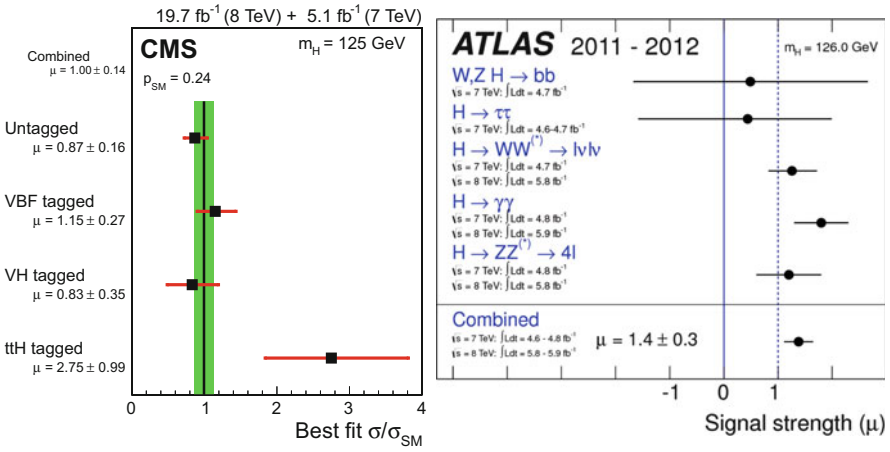

Fig. 3.24 Measured H couplings compared with the SM predictions by the CMS [260] (2016 updated version, included with permission) and ATLAS [66] collaborations (earlier 2013 version, when these lectures were written, included with permission). For a 2016 update of the ATLAS plot, see [3]

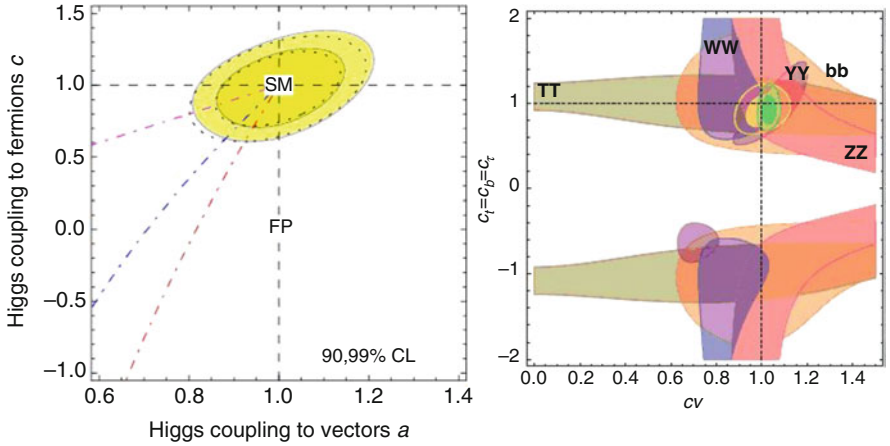

Fig. 3.25 Fit of the Higgs boson couplings obtained from the (unofficially) combined ATLAS and CMS data assuming common rescaling factors a and c with respect to the SM prediction for couplings to vector bosons and fermions, respectively. *Left*: From [218]. *Dashed lines* correspond to different versions of composite Higgs models. The *dashed vertical line*, marked FP (fermiophobic) corresponds to $a = 1$ and $c = 1 - \xi$. Then *from bottom to top* $c = (1 - 3\xi)/a$, $c = (1 - 2\xi)/a$, $a = c = \sqrt{1 - \xi}$, with ξ defined in Sect. 3.17. *Right*: From [194], with $c_t = c_b = c_\tau = c$ and $c_V = a$

turns out to be in agreement with the SM [194]. For example, in the MSSM, at the tree level, $a = \sin(\beta - \alpha)$, for fermions the u- and d-type quark couplings are different: $c_t = \cos\alpha/\sin\beta$ and $c_b = -\sin\alpha/\cos\beta = c_\tau$. At the tree level (but radiative corrections are in many cases necessary for a realistic description), the α

angle is related to the A, Z masses and to β by $\tan 2\alpha = \tan 2\beta (m_A^2 - m_Z^2)/(m_A^2 + m_Z^2)$. If c_t is enhanced, c_b is suppressed. In the limit of large m_A, $a = \sin(\beta - \alpha) \to 1$.

In conclusion it really appears that the Higgs sector of the minimal SM, with good approximation, is realized in nature. Apparently, what was considered just as a toy model, a temporary addendum to the gauge part of the SM, presumably to be replaced by a more complex reality and likely to be accompanied by new physics, has now been experimentally established as the actual realization of the EW symmetry breaking (at least to a very good approximation). If the role of the newly discovered particle in the EW symmetry breaking is confirmed, it will be the only known example in physics of a fundamental, weakly coupled, scalar particle with vacuum expectation value (VEV). We know many composite types of Higgs-like particles, like the Cooper pairs of superconductivity or the quark condensates that break the chiral symmetry of massless QCD, but the Higgs found at the LHC is the only possibly elementary one. This is a death blow not only to Higgsless models, to straightforward technicolor models, and to other unsophisticated strongly interacting Higgs sector models, but actually a threat to all models without fast enough decoupling, in the sense that, if new physics comes in a model with decoupling, the absence of new particles at the LHC helps to explain why large corrections to the H couplings are not observed.

3.17 Limitations of the Standard Model

No signal of new physics has been found, either by direct production of new particles at the LHC, or in the electroweak precision tests, or in flavour physics. Given the success of the SM, why are we not satisfied with this theory? Once the Higgs particle has been found, why don't we declare particle physics closed? The reason is that there are both conceptual problems and phenomenological indications for physics beyond the SM. On the conceptual side the most obvious problems are that quantum gravity is not included in the SM and that the famous hierarchy (or naturalness or fine-tuning) problem remains open. Among the main phenomenological hints for new physics we can list coupling unification, dark matter, neutrino masses (discussed in Sect. 3.7), baryogenesis, and the cosmological vacuum energy. At accelerator experiments, the most plausible departure from the SM is the muon anomalous magnetic moment which, as discussed in Sect. 3.9, shows a deviation by about 3 σ, but some caution should be applied since a large fraction of the uncertainty is of theoretical origin, in particular that due to the hadronic contribution to light–light scattering [245].

The computed evolution with energy of the effective SM gauge couplings clearly points towards the unification of the electroweak and strong forces (GUTs) at scales of energy $M_{\rm GUT} \sim 10^{15}$–10^{16} GeV [315], which are close to the scale of quantum gravity, $M_{\rm Planck} \sim 10^{19}$ GeV. The crossing of the three gauge couplings at a single

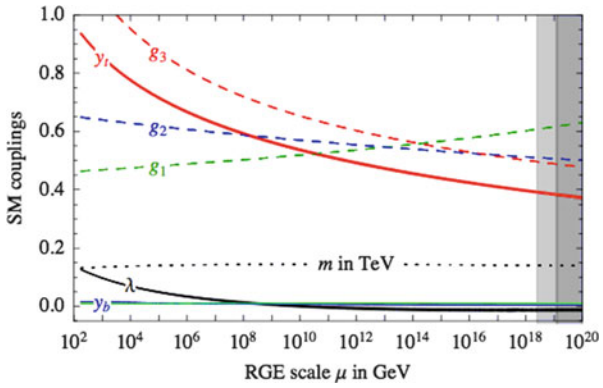

Fig. 3.26 Renormalisation of the SM gauge couplings $g_1 = \sqrt{5/3}g_Y$, g_2, g_3, of the *top*, *bottom*, and τ couplings (y_t, y_b, y_τ), of the Higgs quartic coupling λ, and of the Higgs mass parameter m. In the figure, y_b and y_τ are not easily distinguished. All parameters are defined in the $\bar{M}\bar{S}$ scheme [118]

point is not perfect in the SM and is much better in the supersymmetric extensions of the SM. But still the matching is sufficiently close in the SM (see Fig. 3.26, [118]) that one can imagine some atypical threshold effect at the GUT scale to fix the apparent residual mismatch. One is led to imagine a unified theory of all interactions, also including gravity (at present superstrings [231] provide the best attempt at such a theory).

Thus GUTs and the realm of quantum gravity set a very distant energy horizon that modern particle theory cannot ignore. Can the SM without new physics be valid up to such high energies? One can imagine that some obvious problems of the SM could be postponed to the more fundamental theory at the Planck mass. For example, the explanation of the three generations of fermions and the understanding of fermion masses and mixing angles can be postponed. But other problems must find their solution in the low energy theory. In particular, the structure of the SM could not naturally explain the relative smallness of the weak scale of mass, set by the Higgs mechanism at $v \sim 1/\sqrt{G_F} \sim 250\,\text{GeV}$, where G_F is the Fermi coupling constant. This so-called hierarchy problem [219] is due to the instability of the SM with respect to quantum corrections. In fact, nobody can believe that the SM is the definitive, complete theory but, rather, we all believe it is only an effective low energy theory.

The dominant terms at low energy correspond to the SM renormalizable Lagrangian, but additional non-renormalizable terms should be added which are suppressed by powers (modulo logs) of the large scale Λ, where physics beyond the SM becomes relevant (for simplicity we write down only one such scale of new physics, but there could be different levels). The complete Lagrangian takes the

general form

$$\mathscr{L} = O(\Lambda^4) + O(\Lambda^2)\mathscr{L}_2 + O(\Lambda)\mathscr{L}_3 + O(1)\mathscr{L}_4 + O(1/\Lambda)\mathscr{L}_5 + O(1/\Lambda^2)\mathscr{L}_6 + \cdots \,. \tag{3.128}$$

Here $\mathscr{L}_\mathrm{D}$ are Lagrangian vertices of operator dimension D. In particular $\mathscr{L}_2 = \Phi^\dagger\Phi$ is a scalar mass term, $\mathscr{L}_3 = \bar{\Psi}\Psi$ is a fermion mass term (which in the SM only appears after EW symmetry breaking), $\mathscr{L}_4$ describes all dimension-4 gauge and Higgs interactions, $\mathscr{L}_5$ is the Weinberg operator [363] (with two lepton doublets and two Higgs fields) which leads to neutrino masses (see Sect. 3.7), and $\mathscr{L}_6$ includes 4-fermion operators (among others). The first line in (3.128) corresponds to the renormalizable part (that is, what we usually call the SM). The baseline power of the large scale Λ in the coefficient of each $\mathscr{L}_\mathrm{D}$ vertex is fixed by dimensions. A deviation from the baseline power can only be naturally expected if some symmetry or some dynamical principle justifies a suppression. For example, for the fermion mass terms, we know that all Dirac masses vanish in the limit of gauge invariance and only arise when the Higgs VEV v breaks the EW symmetry. The fermion masses also break chiral symmetry. Thus the fermion mass coefficient is not linear in Λ modulo logs, but actually behaves as $v \log \Lambda$. An exceptional case is the Majorana mass term of right-handed neutrinos ν_R, $M_\mathrm{RR}\,\bar{\nu}_\mathrm{R}^\mathrm{c}\nu_\mathrm{R}$, which is lepton number non-conserving but gauge invariant (because ν_R is a gauge singlet). In fact, in this case one expects $M_\mathrm{RR} \sim \Lambda$. As another example, proton decay arises from a 4-fermion operator in $\mathscr{L}_6$, suppressed by $1/\Lambda^2$, where in this case Λ could be identified with the large mass of lepto-quark gauge bosons that appear in GUTs.

The hierarchy problem arises because the coefficient of $\mathscr{L}_2$ is not suppressed by any symmetry. This term, which appears in the Higgs potential, fixes the scale of the Higgs VEV and of all related masses. Since empirically the Higgs mass is light, (and by naturalness, it should be of $O(\Lambda)$, we would expect Λ, i.e., some form of new physics, to appear near the TeV scale. The hierarchy problem can be put in very practical terms (the "little hierarchy problem"): loop corrections to the Higgs mass squared are quadratic in the cutoff Λ, which can be interpreted as the scale of new physics.

The most pressing problem is from the top loop. With $m_\mathrm{h}^2 = m_\mathrm{bare}^2 + \delta m_\mathrm{h}^2$, the top loop gives

$$\delta m_{\mathrm{h}|\mathrm{top}}^2 \sim -\frac{3G_\mathrm{F}}{2\sqrt{2}\pi^2} m_t^2 \Lambda^2 \sim -(0.2\Lambda)^2 \,. \tag{3.129}$$

If we demand that the correction not exceed the light Higgs mass observed by experiment (that is, we exclude an unexplained fine-tuning), Λ must be close, $\Lambda \sim O(1\ \mathrm{TeV})$. Similar constraints also arise from the quadratic Λ dependence of loops with exchanges of gauge bosons and scalars, which, however, lead to less pressing bounds. So the hierarchy problem strongly indicates that new physics must be very close (in particular the mechanism that quenches or compensates the top

loop). The restoration of naturalness would occur if new physics implemented an approximate symmetry implying the cancellation of the Λ^2 coefficient. Actually, this new physics must be rather special, because it must be very close, while its effects are not yet clearly visible, either in precision electroweak tests (the "LEP paradox" [80]), or in flavour-changing processes and CP violation.

It is important to note that, although the hierarchy problem is directly related to the quadratic divergences in the scalar sector of the SM, the problem can actually be formulated without any reference to divergences, directly in terms of renormalized quantities. After renormalization, the hierarchy problem is manifested by the quadratic sensitivity of μ^2 to the physics at high energy scales. If there is a threshold at high energy, where some particles of mass M coupled to the Higgs sector can be produced and contribute in loops, then the renormalized running mass μ will evolve slowly (i.e., logarithmically according to the relevant beta functions [195]) up to M and there, as an effect of the matching conditions at the threshold, rapidly jump to become of order M (see, for example, [79]). In fact, in Fig. 3.26, we see that, under the assumption of no thresholds, the running Higgs mass m evolves slowly, starting from the observed low energy value, up to very high energies. In the presence of a threshold at M one needs a fine-tuning of order μ^2/M^2 in order to fix the running mass at low energy to the observed value.

Thus for naturalness either new thresholds appear endowed with a mechanism for the cancellation of the sensitivity or they had better not appear at all. But certainly there is the Planck mass, connected to the onset of quantum gravity, which sets an unavoidable threshold. One possible point of view is that there are no new thresholds up to M_{Planck} (at the price of giving up GUTs, among other things) but, miraculously, there is a hidden mechanism in quantum gravity that solves the fine-tuning problem related to the Planck mass [221, 322]. For this one would need to solve all phenomenological problems, like dark matter, baryogenesis, and so on, with physics below the EW scale. Possible ways to do so are discussed in [322]. This point of view is extreme, but allegedly not yet ruled out.

The main classes of orthodox solutions to the hierarchy problem are:

- Supersymmetry [302]. In the limit of exact boson–fermion symmetry, quadratic bosonic divergences cancel so that only log divergences remain. However, exact SUSY is clearly unrealistic. For approximate SUSY (with soft breaking terms and R-parity conservation), which is the basis for most practical models, Λ^2 is essentially replaced by the splitting of SUSY multiplets, $\Lambda^2 \sim m^2_{\text{SUSY}} - m^2_{\text{ord}}$, with m_{ord} the SM particle masses. In particular, the top loop is quenched by partial cancellation with s-top exchange, so the s-top cannot be too heavy. After the bounds from the LHC, the present emphasis is to build SUSY models where naturalness is restored not too far from the weak scale, but the related new physics is arranged in such a way that it would not have been visible so far. The simplest ingredients introduced in order to decrease the fine tuning are either the assumption of a split spectrum with heavy first two generations of squarks (for some recent work along this line see, for example, [271]) or the enlargement of

the Higgs sector of the MSSM by adding a singlet Higgs field (see, for example, [196] on next-to-minimal SUSY SM or NMSSM) or both.

- A strongly interacting EW symmetry-breaking sector. The archetypal model of this class is technicolor, where the Higgs is a condensate of new fermions [332]. In these theories there is no fundamental scalar Higgs field, hence no quadratic divergences associated with the μ^2 mass in the scalar potential. But this mechanism needs a very strong binding force, $\Lambda_{\rm TC} \sim 10^3 \Lambda_{\rm QCD}$. It is difficult to arrange for such a nearby strong force not to show up in precision tests. Hence, this class of models was abandoned after LEP, although some special classes of models have been devised a posteriori, like walking TC, top-color assisted TC, etc. [246] (for reviews see, for example, [275]). But the simplest Higgs observed at the LHC has now eliminated another score of these models. Modern strongly interacting models, like little Higgs models [63] [in these models extra symmetries allow $m_{\rm h} \neq 0$ only at two-loop level, so that Λ can be as large as $O(10$ TeV$)$], or composite Higgs models [223, 258] (where non-perturbative dynamics modifies the linear realization of the gauge symmetry and the Higgs has both elementary and composite components) are more sophisticated. All models in this class share the idea that the Higgs is light because it is the pseudo-Goldstone boson of an enlarged global symmetry of the theory, for example $SO(5)$ broken down to $SO(4)$. There is a gap between the mass of the Higgs (similar to a pion) and the scale f where new physics appears in the form of resonances (similar to the ρ, etc.). The ratio $\xi = v^2/f^2$ defines a degree of compositeness that interpolates between the SM at $\xi = 0$ up to technicolor at $\xi = 1$. Precision EW tests impose $\xi < 0.05$–0.2. In these models the bad quadratic behaviour from the top loop is softened by the exchange of new vector-like fermions with charge 2/3, or even with exotic charges like 5/3 (see, for example, [143, 295]).
- Extra dimensions [62, 314] (for pedagogical introductions, see, for example, [331]). The idea is that $M_{\rm Planck}$ appears very large, or equivalently that gravity appears very weak, because we are fooled by hidden extra dimensions, so that either the real gravity scale is reduced down to a lower scale, even possibly down to $O(1$ TeV$)$ or the intensity of gravity is redshifted away by an exponential warping factor [314]. This possibility is very exciting in itself and it is really remarkable that it is compatible with experiment. It provides a very rich framework with many different scenarios.
- The anthropic evasion of the problem. The observed value of the cosmological constant Λ also poses a tremendous, unsolved naturalness problem [205]. Yet the value of Λ is close to the Weinberg upper bound for galaxy formation [364]. Possibly our Universe is just one of infinitely many bubbles (a multiverse) continuously created from the vacuum by quantum fluctuations. Different physics takes place in different universes according to the multitude of string theory solutions [177] ($\sim 10^{500}$). Perhaps we live in a very unlikely universe, but the only one that allows our existence [61, 220, 318]. Personally, I find the application of the anthropic principle to the SM hierarchy problem somewhat excessive. After all,

one can find plenty of models that easily reduce the fine tuning from 10^{14} to 10^{2}: why make our universe so terribly unlikely? If we add, say, supersymmetry to the SM, does the universe become less fit for our existence? In the multiverse, there should be plenty of less finely tuned universes where more natural solutions are realized and which are still suitable for us to live in them. By comparison, the case of the cosmological constant is very different: the context is not as fully specified as the one for the SM (quantum gravity, string cosmology, branes in extra dimensions, wormholes through different universes, and so on). Further, while there are many natural extensions of the SM, so far there is no natural theory of the cosmological constant.

It is true that the data impose a substantial amount of apparent fine tuning, and our criterion of naturalness has certainly failed so far, so that we are now lacking a reliable argument to tell us where precisely the new physics threshold is located. On the other hand, many of us remain confident that some new physics will appear not too far from the weak scale.

While I remain skeptical I would like to sketch here one possibility of how the SM can be extended in agreement with the anthropic idea. If we completely ignore the fine-tuning problem and only want to reproduce, in a way compatible with GUTs, the most compelling data that demand new physics beyond the SM, a possible scenario is the following. The SM spectrum is completed by the recently discovered light Higgs and there is no other new physics in the LHC range (how sad!). In particular there is no SUSY in this model. At the GUT scale of $M_{\rm GUT} \geq 10^{16}\,$GeV, the unifying group is $SO(10)$, broken at an intermediate scale, typically $M_{\rm int} \sim 10^{10}$–10^{12} down to a subgroup like the Pati–Salam group $SU(4) \bigotimes SU(2)_{\rm L} \bigotimes SU(2)_{\rm R}$ or $SU(3) \bigotimes U(1) \bigotimes SU(2)_{\rm L} \bigotimes SU(2)_{\rm R}$ [98]. Note that, in general, unification in $SU(5)$ would not work because we need a group of rank larger than 4 to allow for (at least) two-step breaking: this is needed, in the absence of SUSY, to restore coupling unification and to avoid a too fast proton decay. An alternative is to assume some ad hoc intermediate threshold to modify the evolution towards unification [224].

The dark matter problem is one of the strongest pieces of evidence for new physics. In this model it should be solved by axions [262, 263, 309]. It must be said that axions have the problem that their mass has to be fixed ad hoc to reproduce the observed amount of dark matter. In this respect, the WIMP (weakly interacting massive particle) solution, like the neutralinos in SUSY models, is much more attractive. Lepton number violation, Majorana neutrinos, and the see-saw mechanism give rise to neutrino mass and mixing. Baryogenesis occurs through leptogenesis [115]. One should one day observe proton decay and neutrino-less beta decay. None of the alleged indications for new physics at colliders would survive (in particular, even the claimed muon $g-2$ [297] discrepancy should be attributed, if not to an experimental problem, to an underestimate of the theoretical uncertainties, or otherwise to some specific addition to the above model [257]). This model is in line with the non-observation of the decay $\mu \to e\gamma$ at MEG [16], of the electric dipole

moment of the neutron [75], etc. It is a very important challenge to experiment to falsify such a scenario by establishing firm evidence for new physics at the LHC or at some other "low energy" experiment.

In 2015 the LHC will restart at 13–14 TeV and in the following years should collect a much larger statistical sample than available at present at 7–8 TeV. From the above discussion it is clear that it is extremely important for the future of particle physics to know whether the extraordinary and unexpected success of the SM, including the Higgs sector, will continue, or whether clear signals of new physics will finally appear, as we very much hope.